UNCLASSIFIED

AD 264 878

UNCLASSIFIED

MATERIALS RESEARCH CENTER

FIRST ANNUAL REPORT

of

RESEARCH SUPPORTED UNDER

CONTRACT SD - 67

of the

ADVANCED RESEARCH PROJECTS AGENCY

of the

DEPARTMENT OF DEFENSE

July 1961

NORTHWESTERN UNIVERSITY
THE TECHNOLOGICAL INSTITUTE
EVANSTON ILLINOIS

FIRST ANNUAL REPORT

on

RESEARCH

Supported under contract SD67

Submitted to:

Advanced Research Projects Agency

of

The Department of Defense

July, 1961

Materials Research Center

The Technological Institute

Northwestern University

Evanston, Illinois

INTRODUCTION

The Northwestern University Materials Research Center was established July 1, 1960 after the awarding to the University of a major contract by the Advanced Research Projects Agency of the Department of Defense for the purpose of conducting a coordinated interdisciplinary-interdepartmental program of basic research and graduate education in materials. The Materials Research Center provides financial support for research conducted by faculty members, their post-doctorates, and their graduate students on the basis of proposals submitted to an administering committee. This first annual report is a compendium of the reports of the individual researches supported with funds derived from the ARPA Contract. In certain instances the research was supported in conjunction with other agencies. In these instances the other agencies are indicated in the individual research reports.

The Materials Research Center Committee gratefully acknowledges the assistance of Dr. Julia R. Weertman in editing this compendium and the assistance of our secretarial staff, Mrs. Clarice Nelson, Mrs. Miriam Burton, and Miss Joan Dean, in its preparation.

Materials Research Center Committee

Arno W. Ewald
Rudolf Frerichs
Pierce W. Selwood
Johannes Weertman
Morris E. Fine, Chairman

TABLE OF CONTENTS

X-ray Studies of Defects in Solids

Project Director: J. B. Cohen
Assistant Professor, Department of Materials Science

SUMMARY

The development of diffraction theory in the last decade has clearly shown that a great deal of information concerning defects in crystalline solids can be obtained through careful examination of the entire diffraction pattern (i.e., the shape of diffraction peaks rather than just their breadths) and diffuse scattering. During the past year, a number of research programs have been initiated here which make use of these techniques. The programs also include the extension of the theoretical treatments.

The method of analysis involves Fourier mathematics; a program suitable for either the IBM 650 or 709 computer, to handle the mathematics involved, was developed and tested.

Principal results of the research so far are outlined below:

A. Effects of Thermal-Mechanical Treatments on Faulting. (This research was partially supported by ONR.)

Studies of faulting in Cu-14 at.% Al, Cu_3Au, Ag-62 at.% Au, and Ag-6 at.% Al alloys showed that:

1. A difference in atomic size between solute and solvent (each having the same valence) increases the fault probability even if there is no hexagonal phase in the phase diagram. Previous studies had shown that valence was an important factor and this was confirmed with the Ag-6 at.% Al alloy.

2. As order increases, the fault probability increases, i.e., the fault energy decreases. This supports a suggestion by Seeger that the fault energy is associated with the interaction of the Fermi surface with the zone boundary of the fault; further support for this idea is found by comparing recent information on fault probability, fault energy, and zone overlap.

3. The annealing out of faults in the Cu-14 at.% Al occurs in two stages. In the first stage, the concentration of stacking faults decreases to a constant level for each temperature. The second stage is associated with recrystallization and here about three-quarters of the stacking faults anneal out. Twin faults are more stable.

4. Twin faults are produced during deformation at room temperature in Cu-14 at.% Al and Cu_3Au.

B. Shock-Loading.

In shock loaded crystals of copper:

1. Twinning is orientation dependent, but the dependence of twinning stress on orientation is greater than that expected from a simple critical resolved twinning stress law.

2. The presence of twins appears to deflect reflected rarefaction waves.

3. Micro-twins were detected.

4. In the range 100-250 kb, the dislocation density increases from approximately 5×10^9 to 5×10^{10} per cm^2.

C. Faulting in Electrodeposits.

A high concentration of twin faults but no stacking faults were found in silver electrodeposited from an argento-cyanide solution. The concentration of these faults increases markedly with decreasing temperature, increasing current density, and on addition of CS_2. As the temperature of plating is decreased, the residual rms micro-strains in different crystallographic directions become more dissimilar.

TECHNIQUES

The development (principally by Warren and his co-workers) of the Fourier analysis of diffraction patterns from materials containing defects has recently been reviewed.[1] The stacking fault probability (α) is determined from the anomalous shift of diffraction peaks; for example, the 111 and 200 decrease in separation. The twin fault probability (β) is found from peak asymmetry, i.e., the 200 peak tails toward low angles. Thus β is found from the Fourier sine coefficients of the series representing the peak. The cosine coefficients from two or more orders of diffraction peaks from a specimen permit the determination of the mosaic size (L) and residual rms micro-strain $\langle \varepsilon_L^2 \rangle^{\frac{1}{2}}$, averaged over various distances (L), in a direction normal to the diffracting planes.

The recorded diffraction peak from a specimen containing defects is a convolution of the effects of the defects and instrumental factors. With the coefficients of the series representing a peak from a well annealed specimen and those from the corresponding peak from a faulted specimen, the instrumental effects may be removed.[2] This calculation carried out by hand takes about six hours, even with Lipson-Beevers strips. L. Schwartz of this group has developed a Fortran program for determining the corrected coefficients with the aid of the IBM 650 or 709. The total calculation time, including the time required to take readings from the diffraction peaks, is reduced to about 2½ hours. R. DeAngelis is now attempting to modify

the program to include calculation of coefficients (sine/cosine) and to store the coefficients from the annealed peak for later use. The completed program will be submitted to the IBM-American Crystallographic Association card file.

A. Effects of Thermal-Mechanical Treatments on Faulting, Supported partially by ONR.

D. Mikkola
M.S. Thesis Research

Previous studies in f.c.c. metals of faulting produced by plastic deformation at and below room temperature have shown that in heavily cold worked metals and alloys (filed at liquid nitrogen temperatures) there can be a very heavy concentration of both twin and stacking faults.[3] The faults in pure metals such as copper and silver anneal out rapidly at room temperature.[3] The data on copper alloys[4] show that as the magnitude of the valence difference between solvent and solute increases, the fault probability for a given concentration increases. However, in general, both a size and a valence difference are present. Examination of this detail[4] indicates that the fault probability is not the same in all copper systems having the same electron to atom ratio; size must be important. Seeger[5] has suggested that the fault energy is controlled by the interaction of the Fermi surface with the appropriate hexagonal Brillouin zone surface.

The purposes of the present investigation are to independently establish the importance of valence difference, size difference, and ordering on the stacking fault probability and to study the results of annealing in an alloy.

Acknowledgements are due to Dr. T. J. Kopponaal for furnishing Cu-14 at.% Al single crystals, to Dr. A. A. Hendrickson for Ag-6 at.% Al single crystals, to Drs. B. Roessler and M. B. Bever for the CuAu, and to Dr. Bever for the Ag-62 at.% Au alloy.

Low temperature deformation was carried out by holding the specimen and file above the vapor from liquid nitrogen (-70 ±15°C) and allowing the filings to fall into the liquid or with the specimen and file immersed in liquid nitrogen. After such deformation the filings were packed into a recess in a hollow brass block under liquid nitrogen and mounted in the x-ray diffractometer adapted for use at low temperatures. For annealing studies, samples were sealed in pyrex and annealed in an oil bath regulated to ±1°C.

Table I gives the determined values for α and β for the various metals and alloys and deformation temperatures studied. From a study of this table it can be seen that twin faults are produced by room temperature deformation in the copper alloys studied. The data for Au, Ag and the value for α for Cu-14.3 at.% Al at room temperature check well with those published previously.[3,4] The value of α for copper is somewhat smaller than published data and was established by repeated measurements. Also, α and β increase with decreasing temperature of deformation and β/α is approximately 2. As

each twin fault has two boundaries, this implies that there are about the same number of twins and stacking faults at all temperatures; since the effective particle sizes measured were found to be essentially the same as those computed from α and β, they are essentially completely determined by the faults.

In the case of Cu_3Au, β does not seem to vary much with temperature, so that above -196°C β/α is greater than 2. This situation probably arises from the greater stability in Cu_3Au of twin faults as compared to stacking faults.

In the Ag-Au alloys (where the order is low compared even to the quenched CuAl or Cu_3Au) the fault probability is a linear function of atomic concentration, whereas in the Cu-Au system there is a definite increase in α and β as compared to either copper or gold for both ordered or quenched Cu_3Au.

In both Cu_3Au and Cu-14 at.% Al the stacking fault probability increases with ordering.

At first thought, one might expect that a highly ordered alloy should have a lower fault concentration than a less ordered state; a stacking fault destroys nearest neighbor bonds in a highly ordered material. However, besides strain energy there is also an important electronic factor. In ordered Cu_3Au a zone inside the f.c.c. Brillouin zone and near the Fermi surface is created on ordering; the Hall effect changes from negative to positive.[6] Thus the density of states near the first f.c.c. zone is decreased. As a result, when there is a high concentration of faults, there is less interaction between the Fermi surface and the hexagonal Brillouin zone. Only very little slip on a given plane is necessary to disorder the plane, but between slip planes the material should still be highly ordered. That this is indeed the fact is indicated by published measurements of strength properties and stored energy in ordered and quenched Cu_3Au; after large deformation at room temperature[7], or in liquid nitrogen[8] these quantities still differ appreciably for the two states. After abrading a Cu-Au alloy with only short-range order, the short-range order is still significant[9]. Furthermore, recent resistivity measurements have shown that the resistivity of ordered Cu_3Au becomes greater than that of the quenched alloy after severe deformation[8]; the excess of 0.1 microhm-cm is in fact accounted for approximately by the greater number of stacking faults in the ordered specimen. With Cu-Al or other terminal solid solutions, decreased Fermi energy comes from the effect of the excess charge on the ion core of the solute, rather than from the presence of an extra zone. Ordering would increase the effect. Any effect of ordering on the dislocation density after deformation would also have to be taken into consideration.

Table II, which is a collection of the available data on fault energy, γ, fault probability, α, and Brillouin zone contact, shows correlation among these quantities.

For example: $\frac{\alpha^{-1}_{\text{r.t.}}}{5} = \gamma = \frac{\alpha^{-1}_{\text{Liq.N}_2}}{3}$.

The effect of annealing on α in cold worked Cu-14 at.% Al is shown in Fig. 1. The process seems to be divided into two stages, as indicated by the data for 220°C. Here, only about one-fourth of the faults anneal out in the first stage, the remainder in the second stage, which appears to be associated with recrystallization. Twin faults ($\beta \cong 0.050$) do not anneal out even after $\frac{1}{4}$ hr. at 250°C.

Concerning the kinetics of the second stage, the analysis of Kuhlmann, Masing, and Raffelsieper[15] appears to fit the data. That is

$$\frac{d\alpha}{dt} = -a \exp \frac{Q(\alpha)}{RT}$$

where $Q(\alpha) = Q_o - c\alpha$, a and c are constants, t = time, T = absolute temperature and R = universal gas constant. Then, if $\alpha = \alpha_o$ when $t = t_o$

$$\alpha(t,T) = \frac{RT}{c} \ln \frac{RT}{ac} + \frac{Q_o}{c} - \frac{RT}{c} \ln(t+t_o)$$

For $t \gg t_o$, α should be a linear function of $\ln t$; this relationship was observed at the two temperatures where the second stage occurred, 220°C and 250°C. (The values of c were 52 and 160 Kcal/g-a for 220 and 250°C, respectively.) The plots extrapolated to about the same point for small values of $\ln t$. By assuming that the variation in $\ln \frac{RT}{ac}$ between 220 and 250°C is negligible, Q_o was evaluated to be 64 ±5 Kcal., in good agreement with data on diffusion in this system[16].

This work will be continued in two main directions. Several systems appear promising to provide additional confirmation of Seeger's theory. Recent data on lattice parameters[17] indicate that the addition of Sn to Au increases the overlap of the Fermi surface. Thus, the fault probability should decrease. Electronic specific heat measurements by Professor Whitmore's group here at Northwestern indicate that as a result of the addition of Cd to Ag the Fermi surface pulls away from the zone boundary. Ordering Ni_3Mn causes the material to become ferromagnetic and the Hall coefficient to change from negative to positive, facts which indicate less interaction of the surface with the zone. Therefore there should be a lower fault energy in ordered Ni_3Mn than in the disordered alloy. Examinations of these systems will begin this summer. It is also quite in line with this theory that the stacking fault energy varies with temperature. Transmission electron microscopy will be employed to investigate this point.

Studies of changes in properties with recovery and recrystallization will be started and correlated with changes in faults, strains, etc., as measured by these x-ray techniques. Such studies should prove fruitful in explaining why different properties change over different temperature ranges during recovery and recrystallization and could also provide data on the specific effect per defect.

B. Shock-loading

R. DeArgelis, M.S. Thesis Research

C. S. Smith[18] has reported that in preoriented copper single crystals subjected to plane shock loads, no twin-like structures appeared at 230 kb, but all orientations except [100] parallel to the shock wave showed these markings at 300 kb. We have continued this work with the aid of the DuPont Explosives Department and found that at 250 kb all directions but [100] showed the markings. At 435 the [100] did "twin". Thus, the twinning stress ratio $\frac{[100]}{[111]} \cong 2$, instead of 1.3 as predicted by the effect of orientation on the critical resolved twinning stress.

In collaboration with Professor J. Weertman of the Materials Science Department, dislocation models for twinning have been considered. For deformation in tension, twinning may result from a stack of faults. For example, all the dislocations in a pile-up might dissociate into Frank sessiles and partials. The additional orientation dependence over that based solely on geometry would then arise from the resistance offered to the partial by other pile-ups. A calculation based on this idea leads to the stress, τ, for twinning in the form:

$$\tau = \frac{\gamma}{2b} + \frac{1}{2}\mu n b \sqrt{N/n}$$

where: γ = fault energy, μ = shear modulus, n = number of dislocations per pile-up, b = Burgers vector, and N = total number of dislocations per cm^2. Recently Venables[19] has proposed a twinning model, based on jogging a single dislocation on successive planes. We are now considering how to test the two models.

Fourier analyses were made of diffraction peaks from some of the crystals. It was found that there is a particle size contribution to line broadening at these pressures, and the particle size in a [110] direction increases with the number of slip systems operative during shock, a fact which suggests that more pile-ups occur in a crystal oriented with [100] parallel to the shock than for other orientations. The residual microstrain was greater in the [100] crystal which did not twin. Also, this orientation undergoes a greater permanent compression than the others when twinning does not occur and when there is no back-up plate to remove reflections. This behavior indicates that the stress waves are deflected and spread out when twins are present.

Dislocation densities calculated from the measured strains were found to be about $5 \times 10^9/cm^2$ in crystals subjected to shocks of 100 kb in the [111] direction and $5 \times 10^{10}/cm^2$ at 435 kb. Evidence of faulting was obtained, and the particle size effect is therefore probably due to faulting, supporting the idea that the markings are twins.

The research on shock loading will be continued under an ONR contract which has just been arranged with the University.

C. Faulting in Electrodeposits

L. Schwartz, Ph.D. Thesis Research.

For some time it has been known that the properties of electrodeposited metals differ from those of annealed metals. No complete x-ray study has been made, although the fact is well known that diffraction lines from electrodeposits are broad, as in a cold-worked metal.

An analysis for Ag deposited from an argentocyanide bath has been carried out. The asymmetry of strains in the different crystallographic directions increases with decreasing temperature of plating, while the subgrain size decreases. Twin faults were found in all plates, their number increasing from one every 100 planes at 23°C to one every 30 planes at 3°C. No stacking faults were found even in plate examined at the low plating temperature. Similar increases in strain and faulting were observed after adding CS_2 to the solution or increasing the current density. Silver plated at 60°C exhibited no line broadening although the line breadth of plate annealed at 60°C after plating at a lower temperature was essentially unchanged by annealing.

As there are strains in the plate, dislocations must be introduced by inclusions or growth conditions. The presence of a trapped molecule with a different size would not cause the strains detected by x-rays.

Further research will involve simpler plating solutions, metals with different fault energies and organic additives with known attractions for metal ions. Transmission electron microscopy and x-ray studies will be made.

The x-ray theory will be extended to include the combined effects of strain and faulting. These problems have, up to now, been treated separately. There can be an effect of directional strains on peak asymmetry.[1]

D. Additional Research Contemplated

It is hoped to begin work in the fall on the liquid-solid transition and on order-disorder reactions.

THESES

1. Effects of Explosive Loading on Copper Single Crystals, R. J. DeAngelis, M.S., January 1961.

2. Effects of Thermo-mechanical Treatment on Faulting in Two Copper Base Alloys, D. E. Mikkola, M.S., May 1961.

PUBLICATIONS

Effects of Thermal-mechanical Treatment on Faults in F.C.C. Alloys, by D. Mikkola and J. B. Cohen, submitted for publication to Trans. AIME.

TALKS

1. Structure of Shock Loaded Single Crystals of Copper, R. J. DeAngelis, and J. B. Cohen, given at:
   a) E. I. DuPont Co. Experimental Station, Wilmington, Delaware, January 30, 1961.
   b) AIME Winter Meeting, St. Louis, March 1, 1961.
2. X-ray Studies of Electro-deposited Silver, L. H. Schwartz and J. B. Cohen, given at:
   a) RIAS, Inc., Baltimore, Md., February 1, 1961.
   b) AIME Winter Meeting, St. Louis, March 2, 1961.
3. Effects of Thermal-mechanical Treatment on Faulting in F.C.C. Alloys, Purdue University's School of Metallurgical Engineering, April 11, 1961.

REFERENCES

1. B. E. Warren, "X-ray Studies of Deformed Metals," Prog. in Met. Phys., 8, (1959), Pergamon.
2. A. R. Stokes, Proc. Phys. Soc., 61, 382 (1948).
3. C. N. J. Wagner, Acta Met., 5, 427, 477 (1957).
4. R. L. Smallman and K. H. Westmacott, Phil. Mag., 2, 669 (1957).
5. A. Seeger, Report of the Conference on Defects in Crystalline Solids, Physical Society, London (1955), p. 328.
6. S. Siegel, Phase Transformations in Solids, Wiley & Sons, Inc., New York (1951), p. 366.
7. J. B. Cohen and M. B. Bever, Trans. AIME, 218, 155 (1960).
8. B. Roessler and M. B. Bever, to be published.
9. P. S. Rudman and B. L. Averbach, Acta Met., 4, 382 (1956).

10. L. F. Vassamilet, Jour. Appl. Phys., 32, 778 (1961).

11. B. E. Warren and E. P. Warekois, Acta Met., 3, 473 (1955).

12. A. Seeger and G. Schoeck, Acta Met., 1, 519 (1953).

13. A. Howie and P. R. Swann, to be published in Phil. Mag.

14. H. Suzuki and C. S. Barrett, Acta Met., 6, 156 (1958).

15. D. Kuhlman, G. Masing and J. Raffelsieper, Z. fur Metallkunde, 40, 241 (1949).

16. L. C. daSilva and R. F. Mehl, Trans. AIME, 191, 155 (1951).

17. T. B. Massalski and H. W. King, Acta Met., 8, 684 (1960).

18. C. S. Smith, "Response of Metals to High Velocity Deformation," Metallurgical Society Conferences, Interscience, New York. Also: Private communication.

19. J. A. Venables, Phil. Mag., 6, 379 (1961).

Table I. Stacking Fault Probability α, and Twin Fault Probability β, in Some Face-Centered-Cubic Metals and Alloys.

Material	Deformation Temperature (°C)	Measuring Temperature (°C)	α	β	β/α
Copper	-196	-165	0.010	0.038	3.8
Cu-14.3 at.% Al (ordered)	-196	-165	0.067	0.097	1.4
	- 70	-165	0.046	0.114	2.5
	20	20	0.035	0.050	1.4
Cu_3Au (ordered)	-196	-165	0.024	---	---
	-196	20 (33 days)	0.015	0.059	3.9 (2.5)*
	- 70	20 (20 days)	0.008	0.049	6.1 (2.6)*
	20	20	0.007	0.048	6.9
Au	-196	-165	0.011	---	---
Au-38 at.% Ag	-196	-165	0.013	---	---
Ag	-196	-165	0.022	---	---
Ag-6 at.% Al	-196	-165	0.036 ±0.005	---	---
	20	20	0.012	---	---

α = stacking fault probability

β = twin fault probability

*α from -165°C used in computing ratio.

Table II. Correlation of Measured Stacking Fault Probabilities (α) with Published Data on Radius of Brillouin Zone Contact and Fault Energy.

Material	α^{-1} 20°C	α^{-1} -196°C	Fault Energy (ergs/cm^2)	Radius of Brillouin Zone Contact‡ (gm-cm/sec)
Copper	167-333[4,10]*	100	38±8[12]*	0.24
Cu-5.7 at.% Al	91[4]*	---	16[13]*	
Cu-14.3 at.% Al	29	15	3[13]*	
Cu-20 at.% Zn	63[11]*	34[3]*	10[13]*	
Cu-35 at.% Zn	26[11]*	18[3]*	6[13]*	
Silver	111[10]*	45	21†[14]*	0.18
Ag-6 at.% Al	80	28	5[13]*	
Gold	209[10]*	90	30†[14]*	0.22

*Reference numbers. Values not referenced taken from this investigation.

†Calculated from data on twinning stress.

‡Taken from R. W. Morse, "The Fermi Surfaces of the Noble Metals by Ultrasonics," in Harrison and Webb, ed., The Fermi Surface, John Wiley & Sons, Inc., New York (1960), p. 214.

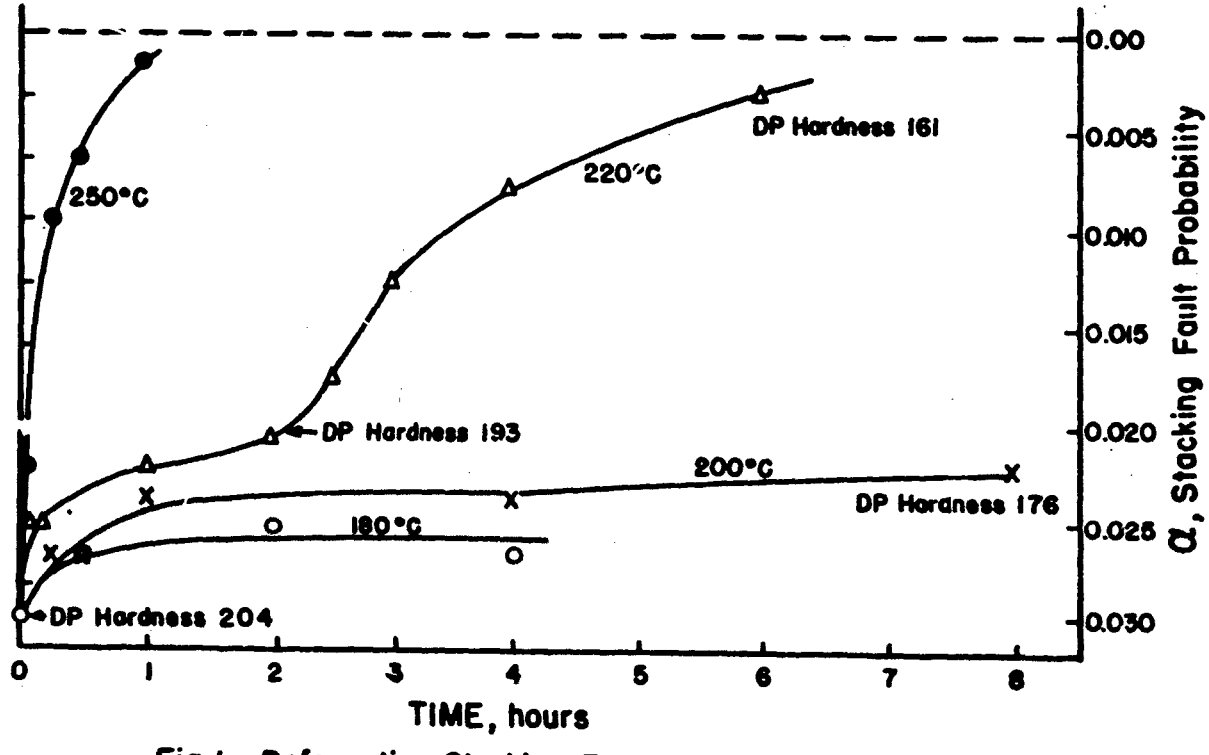

Fig.1—Deformation Stacking Fault Probability α vs. Annealing Time for Cu-14 at.% Al Filed at 20°C

Optical and Electrical Properties of Compound Semiconductors

Project Director: R. J. Cashman
Professor, Department of Physics

C. R. Kannewurf
Postdoctoral Research Associate

This research is partially supported by the U.S. Navy Bureau of Ships.

The principal research of this group has been the preparation of various germanium chalcogenide compounds and the investigation of some of their physical properties. The emphasis in this program has been directed toward studying anisotropic materials with interesting optical properties such as dichroism, birefringence, infrared photoconductivity, and selective absorption characteristics having a wide range of cut-on and cut-off frequencies. Since several materials have been under investigation, the following summary of results will be given by individual compounds.

A. Germanium Monoselenide, GeSe.

Research on this compound was carried on as a continuation of measurements that already were in progress prior to the ARPA program. A complete summary of the optical measurements has been made in a paper entitled, "Optical Absorption and Photoconductivity in Germanium Selenide," which has been accepted for inclusion in the program of the International Conference on Photoconductivity to be held at Cornell University in August, 1961. The papers presented will subsequently be published in the proceedings of the conference. The following paragraph is a summary of the abstract from the submitted paper.

Optical absorption was investigated in extremely thin single crystal specimens of GeSe. Absorption data at 300°K cover a wavelength range of 1.20 to 0.45 microns with the absorption coefficient changing from 30 to 1.2×10^5 cm^{-1}. The GeSe absorption curve is shown in Fig. 1 and also the corresponding curve for germanium sulfide which will be discussed in the next section. An analysis of the absorption edge for direct and indirect transitions is described. In the high absorption region a direct transition photon energy dependence of $(h\nu - E_g)^{3/2}$, with $E_g = 1.53$ ev was shown to give a good fit to the data over a considerably greater energy range than the relation $(h\nu - E_g)^{1/2}$. The spectral response curve for an evaporated film type photoconductive layer of GeSe was obtained in the same wavelength range and is shown in Fig. 2. This curve shows two bands of responsivity with the threshold energies corresponding closely to the energy gap values that were determined for the direct and indirect band transitions.

B. Germanium Monosulfide, GeS.

In view of the analysis of the optical data for GeSe similar measurements already completed for GeS were re-evaluated (C. R. Betz, Ph.D. Thesis, Northwestern University, 1950; unpublished). The result is that GeS has been shown to be similar in most respects to GeSe in the behavior of the optical properties. A comparison of the absorption curves in Fig. 1 shows that they are nearly identical with that of GeS displaced toward higher energies by approximately 0.39 ev. A revised paper entitled "Optical and Electrical Properties of Germanium Sulfide" is now in preparation.

Since GeS and GeSe are highly anisotropic materials, three dimensional crystals are necessary in order to obtain a complete set of galvanomagnetic coefficients to describe the electrical properties. Consequently, techniques are now being considered for the preparation of larger single crystal specimens. Additional optical work on these materials is also being considered. Since Ge is isotypic with GeSe, it may be possible to alloy the two in various proportions in order to control the width of both the direct and indirect energy band gaps. Such a procedure but with different materials has been reported chiefly from Russia.

C. Germanium Disulfide, GeS_2 and Germanium Diselenide, $GeSe_2$.

As reported in the literature, GeS_2 was found to exist in both a crystalline and a vitreous phase. Measurements thus far have been confined to the vitreous GeS_2, which is an amber colored glass. Preliminary transmission data indicate the material is transparent to radiation in a wavelength range of 0.4 to 10.0 microns. Further work on GeS_2 is in progress.

Also prepared and under investigation is $GeSe_2$. Indications are that $GeSe_2$ may also exist in more than one phase; however, all material prepared to date appears to be crystalline. The compound $GeSe_2$ is virtually unknown in the literature.

D. Other Ge - IV_b Compounds.

Polycrystalline ingots of germanium telluride, GeTe, have been prepared but attempts to grow single crystal samples by the methods employed with GeS and GeSe have not been successful. It is known that GeTe has a crystal structure which differs from that of GeS and GeSe, and therefore it is suspected that GeTe will not exhibit similar optical properties.

Several methods have been tried to prepare germanium monoxide, GeO. Considerable disagreement can be found in the literature as to the existence and the exact nature of this di-valent oxide of germanium. From an examination of the samples prepared thus far it is not yet possible to determine whether or not a stable crystalline or vitreous phase of stoichiometric GeO can be prepared. Further work is planned.

PUBLICATIONS

1. Optical Absorption and Photoconductivity in Germanium Selenide, by C. R. Kannewurf and R. J. Cashman submitted to International Conference on Photoconductivity to be held at Cornell University in August, 1961.

2. Optical and Electrical Properties of Germanium Sulfide, by C. R. Betz, C. R. Kannewurf and R. J. Cashman. It is tentatively planned to submit this to The Physics and Chemistry of Solids.

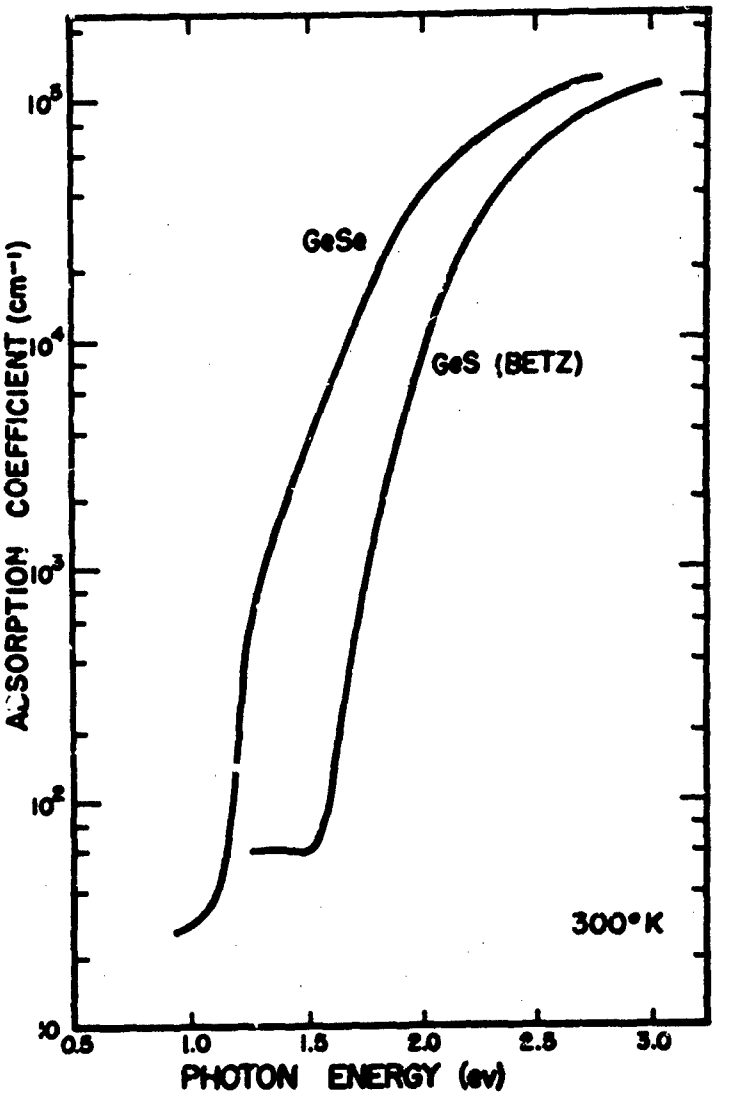

Fig. 1 — Optical Absorption Curves for GeSe and GeS vs Photon Energy

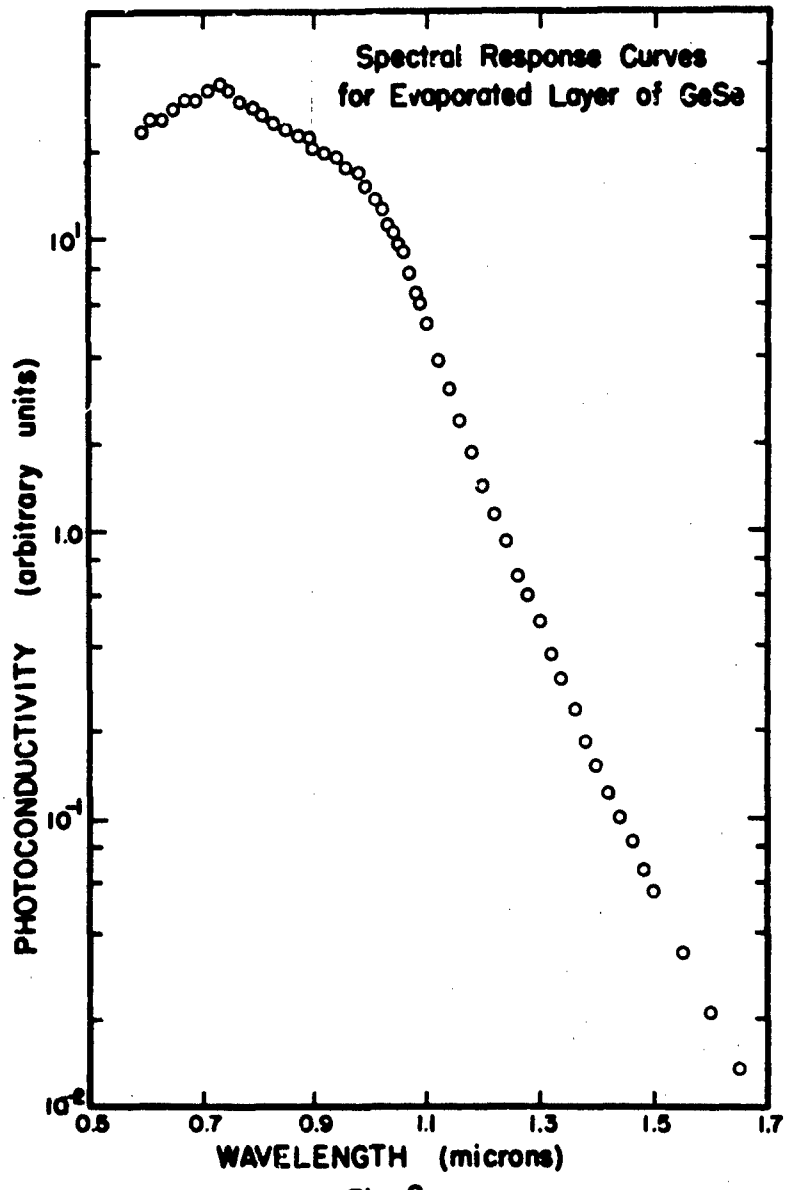
Spectral Response Curves
for Evaporated Layer of GeSe
PHOTOCONDUCTIVITY (arbitrary units)
10¹
1.0
10⁻¹
10⁻²
0.5
0.7
0.9
1.1
1.3
1.5
1.7
WAVELENGTH (microns)

Fig. 2

Materials Research Project #3

Ultra Thin Layers of Metal Single Crystals

Project Director: R. L. Hines
Assistant Professor, Department of Physics

R. Waller
Graduate Research Assistant

The experimental approach to making metal crystals perhaps as thin as one atom is proceeding in two stages. First, the growth of very thin evaporated gold films on a clean mica surface is being investigated. Second, the thinning by thermal evaporation or surface diffusion of the thinnest single crystals which can be detached from the mica will be investigated. At present, an all glass, bakeable vacuum system with a mercury diffusion pump and two liquid air cooled traps is used for the evaporations. The glass evaporator tube is cracked and resealed for each evaporation by the use of standard glass blowing techniques. Bakeable metal flanges and a bakeable valve have been pruchased but have not yet been installed. The mica is cleaved inside the vacuum system just before evaporation to insure a clean mica surface. An estimate of the thickness of the film is obtained from its optical reflection coefficient by extrapolating known data to the very low thicknesses of interest here. It is estimated that a monolayer of gold on mica will reflect 2.5% more light than a mica surface alone.

Approximately twenty-five evaporations of gold on a freshly cleaved mica surface have been carried out at pressures of 10^{-7} mm Hg to 10^{-8} mm Hg and at evaporation rates of 5 Å/min to 500 Å/min. The following phenomena have been observed: a) A 300 Å thick film grown on a heated mica substrate separates from the substrate on cooling over areas 1 mm in diameter so that it should be possible to mount the film independently of the mica. b) When the 300 Å thick film mentioned above is fractured by pulling part of it off with a piece of Scotch tape, it fractures in a pattern consisting predominantly of straight edges intersecting at angles of 60° and 120°. From other work it is expected that the gold film is so oriented that its (111) face, which has hexagonal symmetry, lies parallel to the mica surface. c) On films only a few atoms thick, the reflection coefficient has different values at different points on the surface; striations are formed even though the deposition conditions are uniform. This suggests that the deposited gold atoms diffuse over the surface until they are trapped at steps on the film surface. d) The average width of the striations is 0.01 mm at an estimated mica temperature of 250°C and a deposition rate of 20 Å/min and is 0.07 mm at an estimated mica temperature of 330°C and a deposition rate of 20 Å/min. e) No striations have been seen on films with an average thickness as estimated from the reflection coefficient of two atom layers or less. This suggests that the diffusion coefficient of gold on mica is noticeably less than the diffusion coefficient of gold on

gold. Some of these observations have been presented in a paper at the Washington meeting of the American Physical Society.

In the next year it is planned to make quantitative measurements of the reflection coefficient with a space resolution of 0.005 mm. If such measurements show that the observed striations correspond to discrete values of the film reflection coefficient, it will suggest that the films are exact integer thicknesses of atoms. It is expected to make an electron diffraction study in order to obtain confirmation of the crystallinity of the films. The most promising method of obtaining monolayer foils free of any substrate now appears to be the thinning of foils several hundred Angstroms thick by surface diffusion. An experiment is now being planned to use the electron beam in an electron microscope both to heat the foil to cause surface diffusion and to examine the foil as it is being thinned.

TALKS:

1. R. L. Hines, "Gold Crystals One Atom Thick", Bulletin, American Physical Society II-6 (1961) p.243.

Experimental Determination of Fermi Surfaces in Metals

Project Director: J. A. Marcus
Associate Professor, Department of Physics

This Research is Partially Sponsored by The National Science Foundation

A. Galvanomagnetic Coefficients of Gallium Single Crystals at 77°K[1]

W. A. Reed
Ph.D. Thesis Research

The eighteen components of the magnetoresistivity tensor necessary to specify the relation between the electric field and current in the presence of a magnetic field have been measured at 77°K in fields up to 5 kilogauss. An attempt is being made to analyse the data on the assumption that at these temperatures the Fermi surface can be approximated by a number of suitably chosen ellipsoids. No further work at low magnetic fields is contemplated.

B. Galvanomagnetic Properties of Gallium at Helium Temperatures

W. A. Reed
Ph.D. Thesis Research

Measurements on the magnetic field and orientation dependence of the magnetoresistance, Hall effect, planar Hall effect and quadratic Hall effect have been completed for all orientations in which the current is along a crystallographic direction and the field lies in a principal plane. It appears that the extremely complicated angular dependence of the magnetoresistance may be accounted for by an open Fermi surface. An attempt is being made to analyse the data in terms of a Harrison-type OPW model of the Fermi surface which has been calculated using the 4.2°K values of the lattice parameters of gallium (originally extrapolated from room temperature values but recently confirmed by measurements at 4.2°K by C. S. Barrett of the University of Chicago).

As a general check of the conclusions resulting from this analysis, additional measurements will be made at orientations in which the current is not limited to axial directions. These measurements should provide a better understanding of the quadratic Hall effect, which has also been observed in tin[2] and copper[3].

C. The De Haas-Van Alphen Effect

J. Condon
Ph.D. Thesis Research

In order to supplement the information on the Fermi surface of gallium obtained from the above galvanomagnetic measurements, a detailed study of the de Haas-van Alphen effect has been initiated. Measurements are performed with a servo-type recording torsion balance of sensitivity 2×10^{-4} dyne cm/mm. With this improved instrument obtaining data has become almost a trivial matter but the complexity of the data is such that its reduction has become the major problem to be solved.

The recording torsion balance has been used to study the dH-vA effect in calcium at 1.3°K. The dominant period, $P = 2.9 \times 10^{-7}$ gauss^{-1}, is five times that observed by Berlincourt[4]. This discrepancy must arise from the fact that we are studying a different portion of the Fermi surface than that which gives rise to the short period oscillations observed by the high pulsed field-technique. Detailed investigation of calcium awaits the installation of the large ADL magnet.

Investigation of other metals of interest (beryllium and zinc alloys in particular) will be undertaken as single crystal samples become available.

D. Magnetic Susceptibility of Dia- and Paramagnetic Substances

As a result of Janninck and Whitmore's observation of an anomaly in the electronic specific heat of a series of α-AgCd alloys, susceptibility measurements were made on their samples at room and liquid helium temperatures. No corresponding anomaly in the susceptibility was observed nor was any evidence found of ferromagnetic impurities.

A high sensitivity recording susceptibility balance of the translational type is being constructed to facilitate measurements such as the above.

REFERENCES

1. W. A. Reed and J. A. Marcus, Bull. Am. Phys. Soc. Ser. II, 6, 27 (1961).
2. V. F. Kachinskii, Doklady Akad. Nauk. SSSR 135, 818 (1960).
3. J. R. Klauder and J. E. Kunzler, Phys. Rev. L. 6, 179 (1961).
4. T. G. Berlincourt, Proc. 7th Int. Conf. Low Temp. Phys. p221 U. Toronto Press (1960).

Applications of Interferometry to Dimensional Changes in Solids

Project Director: E. R. Peck
Associate Professor, Department of Physics

Two subdivisions of the project are considered in this report. The first is the measurement of magnetostriction in paramagnetic or diamagnetic materials. This research is well under way. The second subdivision is being planned concurrently and is the measurement of creep of solid materials under very low stress.

A. Magnetostriction

N. C. Anderholm
Ph. D. Thesis Research

In 1932 Kapitza[1] published work on magnetostriction in paramagnetic and diamagnetic materials. He observed magnetostriction in bismuth, antimony, graphite and gallium, the largest effect being in bismuth. Schoenberg[2], working under Kapitza's direction at a later time, did additional work which first allowed determination of the complete set of magnetostriction moduli of bismuth. Probable errors in Kapitza's and Schoenberg's work were of the order of 10%. The same precision was realized by Wolf and Goertz[3], who investigated the effect of impurities on the magnetostriction of bismuth, although their purest material was 99.97% bismuth. Interferometric techniques should now permit measurement of length changes one hundred times smaller than those measurable by Kapitza. It is proposed first to repeat work on bismuth, with expected precision of the order of 2%, and with material of present standards of purity. Other materials may then be investigated.

Instrumentation is in the final stages of development. The dilatometer contains a Michelson interferometer using corner prisms for stability of optical adjustment.[4] A photomultiplier views the interference fringes formed by green light from a mecury arc, while a second photomultiplier monitors the arc. These two photocells and their associated amplifiers form with the interferometer a combined optical and electrical bridge circuit, which is unbalanced by differential motion of the two corner prisms. An output meter reads the unbalanced signal. Effects of arc variation, supply voltage variation, and thermal expansion of the interferometer as a whole are minimized by this bridge arrangement. Coupling between the interferometer and the sample is made by the motion of diaphragms in a closed hydraulic system, which is designed to magnify the dilatation of the sample by a factor of ten while transmitting it to the interferometer. The hydraulic system is balanced against thermal expansion of the fluid. Such a coupling system has the advantage of freedom from static friction. It permits various orientations of the sample between magnet poles, while the interferometer remains outside the field. Ultimate sensitivity of the entire dilatometer is expected to be about three Angstrom units for full-scale deflection of the meter.

The longitudinal strain $\Delta l/l$ of a rod subjected to a longitudinal magnetic field H has been shown[3];[5] to be expressible in the form

$$\Delta l/l = -\frac{1}{2} H^2 \left[\frac{\partial X}{\partial p} + \frac{X}{Y(1-2\sigma)}\right]$$

where X is the susceptibility of the material, p is longitudinal stress, Y is Young's modulus and σ is Poisson's ratio. Previous investigators of magnetostriction in bismuth were not able to observe the second term in the square brackets because of the probable error in their work. Dependence of the whole quantity in square brackets upon H has been proposed for ferromagnetic materials[6], and is suggested for bismuth by the data of Wolf and Goertz[3], but not by the data of Kapitza or Schoenberg.[1,2] This is a question which needs clarification by more precise measurements.

B. Creep Under Low Stress

Baij Nath Khanna, Postdoctoral Research Associate

The ability of interferometric techniques to measure dilations of only thirty Angstrom units with some accuracy, and to observe down to perhaps a hundredth of this quantity, suggests the use of these means for observing strains under very small stress. In the low-temperature range for pure crystals, creep sets in at small stresses as a result of the motion of dislocations. It is proposed to construct an interferometer of particularly great stability, in a thermostatically controlled housing, to observe creep near room temperature. Work of Chalmers[7] on this microcreep in tin may then be checked and extended to other materials. An interferometer of the type described would have other uses as well, for example in a study of recovery after irradiation.

REFERENCES

1. P. Kapitza, Roy. Soc. Proc. A 135, 537 (1932)
2. D. Schoenberg, Roy. Soc. Proc. 150, 619 (1935)
3. Wolf and Goertz, Phys. Rev. 46, 1095 (1934)
4. Peck and Obetz, J. Opt. Soc. Am. 43, 505 (1953)
5. Holmholtz, Ann. d. Phys. 13, 385 (1881)
6. A. Gusev, Zh. Eksp. Teor. Fiz. 29, 2(8), 181 (1955)
7. B. Chalmers, Proc. Roy. Soc. A 156, 427 (1936)

Studies of Semiconducting Gray Tin, Supported partially by ONR

Project Director: A. W. Ewald
Associate Professor, Department of Physics

H. J. Lauc
Research Assistant

A. Purification of Tin and Growth of Gray Tin Crystals

An investigation of two new methods of purifying tin has yielded some very encouraging results. In the first of these methods, which has the advantage of a relatively high yield of purified material, gray tin crystals and crystals of $HgSn_{12}$ are grown simultaneously from mercury solution. Impurities are concentrated in the gray tin, which is discarded. The compound is redissolved and gray tin crystals are grown from the solution. This method has produced crystals having an impurity concentration of 7×10^{15} per cc as compared with the 3×10^{16} per cc of the best commercial tin (which, incidentally, has only recently become available). In the second method mercury is absorbed by chunks of gray tin as the temperature is raised above 0°C. This mercury is expelled at lower temperatures and carries with it tin that is quite free of impurities. The method has a low yield and only two samples have been tested thus far, but the better of these contained only 6×10^{14} impurity atoms per cc. In comparison with the tin used in our previous studies of semiconducting properties, this represents an improvement of two orders of magnitude. It is remarkable that crystals of this purity can be grown from mercury solution. It appears that the solubility of mercury in gray tin (at sufficiently low temperatures) is extremely small. This is a most fortunate circumstance for the further investigation of the semiconducting properties since growth from mercury solution is the only method of obtaining single crystals.

Future work on purification will emphasize the second method in order to accumulate a more adequate supply of the highest purity material. The first method will be used to produce lightly-doped, n-type material.

B. Semiconducting Properties of Gray Tin

R. E. Lindquist
Ph.D. Thesis Research

E. D. Hinkley
Research Assistant

A renewed investigation of photoconductivity with the higher purity specimens and a new helium dewar designed for optical work is in progress. Previously the photo-sensitivity was insufficient to observe the spectral

response. In a preliminary experiment under the new conditions a response to monochromatic infrared radiation was detected out to 16.5 microns at liquid helium temperature. Further measurements to determine the relative spectral sensitivity, the absolute sensitivity and the dependence of the long wavelength limit upon temperature and purity are planned for the immediate future.

A study of the optical properties of gray tin through measurements of the reflectivity of a natural surface to monochromatic, polarized infrared radiation has been in progress for several years. During the past year final room temperature data have been obtained. The wavelength dependence of the absorption coefficient and of the index of refraction have been determined in the region from 1 to 25 microns. The refractive index has a constant value of 4.75 in the 1 to 6 micron region and then decreases to approximately 1.5 at 22 microns. The absorption coefficient decreases from 3×10^5 cm^{-1} at 1 micron to 8×10^3 at 15 microns and then rises again at longer wavelengths. The measurements are now being extended to lower temperatures and to doped material in order to isolate the individual effects of electrons and holes on the optical properties.

Closely related to the photoconductivity and reflectivity measurements is a study of the infrared transparency. All previous searches for transparency at long wavelengths have yielded negative results, presumably because of strong free carrier absorption. However, in view of the marked improvement in purity that has been achieved, a reinvestigation seems justified and will be undertaken. Techniques for grinding specimens to thicknesses of the order of 10 microns without converting them to metallic tin have already been worked out and the equipment necessary for transmission measurements at low temperatures is at hand.

A search for magneto-plasma reflection in which the application of a magnetic field produces a splitting of the minimum in the normal reflectivity curve was undertaken during the past year. No effect on the reflectivity of gray tin of magnetic fields up to 25 kilogauss was observable in "pure" samples or in specimens doped with up to 10^{19} impurity atoms per cc.

Preparations are under way for cyclotron resonance experiments to be performed in collaboration with Dr. Dexter of the University of Wisconsin. The special problems of handling gray tin and of mounting specimens in the resonant cavity have been discussed and the first experiments are planned for June.

Materials Research Project #7

Work Function Phenomena in Solids

Project Director: R. Frerichs
Professor, Department of Electrical Engineering

R. Handy
Ph.D. Thesis Research

A. Tunnelling Phenomena in Thin Insulating Films

An investigation of the phenomenon of tunneling through thin insulating films is underway. Several hundred samples were prepared by evaporating aluminum on carefully cleaned glass slides, oxidizing the aluminum, and then evaporating another layer of aluminum or other metal on top of the oxide. Both anodic oxidation and heating in dry oxygen were tested as methods for producing the oxide layer; the effects of tempering the oxidized layers in vacuum prior to the second evaporation were studied. The following behavior was observed.

1) All samples show symmetrical I-V characteristics typical of tunnel conduction, with surface resistivity roughly controllable from 10^{-2} ohm cm^2 to 10^7 ohm cm^2, the value dependent upon the particular treatment. No significant amount of rectification was observed.

2) The I-V characteristics of a group of samples whose initial films were prepared and oxidized all at the same time are profoundly affected by the intensity and duration of vacuum tempering prior to the second evaporation. The longer the tempering and the higher the temperature, the lower the resistivity of the resulting barriers.

It was also observed that the characteristics of the junction and particularly the uniformity of the oxide films depends critically upon the vacuum maintained during the second evaporation. All the above-mentioned samples were prepared in a standard vacuum coating stand evacuated by a water baffled oil diffusion pump capable of maintaining the pressure in the bell jar at 1×10^{-5}TOR. This pressure range represented a serious limitation since the tunneling junctions are observably dependent on gaseous contamination introduced during the evaporation. In order to overcome this limitation an all glass, a bakeable ultra-high vacuum evaporation system was designed which utilizes a mercury diffusion pump and liquid nitrogen traps. This system has just been completed and has undergone preliminary tests which show that it is capable of reaching static pressures in the evaporation manifold of 10^{-10}TOR after bakeout, and of holding at 5×10^{-6}TOR or less during the actual evaporation. At this writing, the first few samples which have been produced show that the tunnel resistance is still sensitive to the tempering time and temperature, a behavior which indicates that this phenomenon is affected by gradual changes in the structure of the metal-oxide layers, and that it is

probably independent of the residual pressure during evaporation. During the coming quarter, the much improved vacuum conditions will be used to study this phenomenon: factors governing the uniformity of the tunnel junctions, and the influence of electron state density and work function of the electrode metal.

B. Work Function Studies at Very Low Temperatures.

An ultra sensitive detector for measuring work function changes at very low temperatures by the CPD method was constructed. The sensing element is a vacuum encapsulated vibrating capacitor which can be immersed in liquid helium. In order to avoid electrical pickup and cool-out loss from driving the capacitor, a resonant molybdenum reed was utilized. When cooled the mechanical Q of the reed is so high that it can be excited at resonance by an external generator mechanically coupled to the frame supporting the helium dewar. To overcome the serious noise problems generated by the boiling coolant and stray electrical pickup an auto-correlator was included in the measuring circuit, with integration time variable from seconds to minutes. The completed unit had an input impedance greater than 10^{14} ohms and was capable of detecting voltage in CPD changes of less than 0.0005 volts.

The unique sensitivity of this device was used to investigate the theoretical predictions that the energy gap associated with the onset of superconductivity grows symmetrically around the Fermi level. The theoretical expectations were confirmed and no change in work function was observed to be associated with superconductivity.

Studies of Dislocations in Solids

Project Director: J. Weertman
Associate Professor, Department of Materials Science

A. Investigation of the Incubation Creep Effect

R. Arsenault
Ph. D. Thesis Research

This project is concerned with an investigation of the incubation creep effect in alpha iron. Since the first observation of the incubation effect in alpha iron[1] no further attempts have been made either to explain its origin or to obtain more experimental data on its behavior. It is planned to treat both these aspects of the problem in this study.

The incubation effect occurs in alpha iron when a small stress increment is added to a sample which is under a tensile stress and is at a temperature of the order of 20° to 100°C. After the addition of the stress increment the sample first deforms at a very slow rate but, after a time interval (the incubation time), the rate of deformation suddenly increases. Later the deformation rate slows down again and approaches zero. If another stress increment is added after the rate has become zero the whole incubation effect is repeated.

The samples used in this investigation are made from high purity iron* with an interstitial content of 10-20 ppm. The iron is polycrystalline with an average grain dimension of about 5 mm.

A portion of a stress increment test is plotted in Fig. 1. The initial stress(2.6 Kg/mm^2) was 3/4 of the yield strength. The first stress increment was added about two hours later. After this addition the samples elongated at a constant but very slow rate. After an incubation time the rate of deformation increased. The incubation time varies with temperature and with the magnitude of the stress increment. The time interval during which rapid deformation occurs also is a function of these variables. Further, the incubation time is a function of an "aging" time, where the aging time is defined as the time interval between the end of the rapid deformation and the addition of a new stress increment to start anew the incubation effect. The incubation effect can be repeated from 20 to 40 times before a sample fractures.

---

*Zone refined iron supplied by Battelle Memorial Institute. We are indeed indebted to Mr. James W. Halley, Chairman of the Subcommittee for High Purity Iron of the American Iron and Steel Institute, for his aid in obtaining samples of this iron.

The relationship between aging time and incubation time is shown in Fig. 2. As the aging time is increased the incubation time increases. It can be seen from Fig. 2 that the effect of an increase in temperature is to reduce the length of the incubation time.

One might expect that temperature has two contradictory influences on the incubation phenomenon. It is known from Fig. 2 that a relatively high specimen temperature aids whatever process is leading to the onset of rapid deformation. However, again from Fig. 2, it can be seen that a long aging time increases the length of the incubation period and thus delays and hinders whatever mechanism causes the rapid deformation. Since the aging phenomenon probably involves some sort of diffusion process, an increase in aging time can be expected to be equivalent to an increase in temperature. Tests have been conducted in an attempt to sort out these two temperature effects. For example, a series of experiments were carried out in which samples were always aged at the temperature 50°C while incubation time was measured at 30°, 40°, and at 50°C. It was found that the incubation time determined from these tests obeys a law of the type

$$t = A \exp (Q_i/RT) \qquad (1)$$

where t is the incubation time, A is a constant (for a fixed aging time and aging temperature), Q_i is an activation energy, R is the gas constant, and T is the temperature during the incubation period. An activation energy of 20,000 cal/mole was determined from these experiments.

It is planned to carry out a complementary experiment in which the incubation time is measured at a fixed temperature but the aging is carried out at various temperatures. If the aging phenomenon is diffusion controlled, an aging time τ_1 at temperature T_1 can be related to an aging time τ_2 at a temperature T_2 through the equation

$$\tau_1 \exp (-Q_a/RT_1) = \tau_2 \exp (-Q_a/RT_2) \qquad (2)$$

where Q_a is the activation energy connected with the aging process.

Although Q_a has not yet been measured by means of this complementary experiment, its value has been determined by a less direct method. Samples have been tested at a number of different temperatures but with no temperature change made between the aging and the incubation part of the creep curve. Now if one knew the value of Q_a, it would be possible with the aid of Eq. (2) to translate the aging time at any particular temperature. In addition, if the length of the aging time at any given temperature were chosen so that the equivalent time at the reference temperatures is always the same, Eq. (1) could be used to determine the incubation activation energy. Since Q_a is not known initially one can only make a guess at its value. If the guess is incorrect, the value of Q_1 which is obtained will differ from the value of 20,000 cal/mole found by direct testing. If the value of Q_a is guessed correctly, the calculated value of Q_1 will agree with the directly measured value of this quantity. Since it was suspected that carbon diffusion is responsible for the aging effect we picked a value of Q_a equal to 20,000 cal/mole, the diffusion activation energy of carbon in alpha iron. This value of Q_a leads to an incubation activation energy whose value also is 20,000 cal/mole, in agreement with the value measured by the direct experiment. Hence, we find that Q_a is equal to 20,000 cal/mole.

The curve of incubation time versus aging time for tests made entirely at one temperature follows a law of the type:

$$t = c\tau^n \tag{3}$$

where n is a constant of the order of 1/2 to 3/4, and c is another constant.

In the incubation period a sample elongates at a constant, but slow, strain rate $\dot{\varepsilon}$. This strain rate increases as a result of an increase in the stress increment applied to the sample and diminishes with an increase in the length of the preceding aging period. The strain rate is related to aging time by the equation

$$\dot{\varepsilon} = c'\tau^{-n} \tag{4}$$

where c' is a constant and n is the same constant appearing in Eq. (3). Thus one finds that the incubation strain $\dot{\varepsilon}$ and the incubation time are inversely proportional to each other.

The aging time has no influence on the length of the time interval during which rapid deformation occurs nor does it have any effect on the total strain which occurs within this time interval. However, both the rapid deformation time and the total rapid deformation strain are functions of stress and temperature. It was found that the relationship between rapid deformation time and temperature can be expressed by an equation of the type of Eq. (1) in which the activation energy ranges from 12,400 to 17,000 cal/mole. The actual value of the activation energy depends on stress. Its value extrapolated to zero stress is 24,400 cal/mole.

The explanation of the incubation creep effect obviously will be complex since several processes are involved in the phenomenon. The theory proposed by van Buren[2] to explain a somewhat similar incubation effect in germanium will not work for alpha iron. We are attempting to explain the phenomenon in alpha iron in the following manner. We assume that during the aging period before a stress increment is applied, carbon atoms diffuse to dislocation lines and form atmospheres about them. After a stress increment is applied some dislocation sources become active and send out dislocation loops. Because of the carbon atmospheres the dislocations are not free to move on their slip planes but have to drag an atmosphere with them. In this situation the deformation rate is constant but it is slow. This is the incubation period. As a dislocation loop expands, its length increases and the concentration of its atmosphere per length of dislocation line decreases. In time the dislocations are essentially free of their carbon atmospheres and the dislocations move freely on the slip planes. When this situation occurs the elongation rate is fast. This is the rapid deformation region. Finally the rate slows down as a result of such mechanisms as jog formation, dislocation interaction, etc.

REFERENCES

1. M. Gensamer and R. F. Mehl, Trans. AIME, 131, 372 (1938).

2. H. G. van Buren, Physica, 25, 775 (1959).

B. Deformation of Metals at High Strain Rates

J. McCloud
Ph.D. Thesis Research

The purpose of this project is the study of the effect of high strain rates on the deformation of metals. High strain rates will be obtained by impacting samples with a projectile fired from an air gun. A high velocity air gun has been designed to produce projectile velocities up to 500 ft/sec. This gun is now being constructed. The diameter of the projectile that will be fired is 3/4 of an inch and its length is one inch. It will be accelerated down a barrel 14 feet long and will develop an energy of about 480 ft-lbs with the use of an air reservoir of 90 psi pressure. A schematic diagram of the air gun is shown in Fig. 3.

Once the air gun is completed it will be used to study mechanical twinning and the effect of high strain rates on the stress-strain curves of metal single crystals.

C. Internal Friction of Mercury

N. Lalwaney
M.S. Thesis Research

Internal friction measurements are being attempted on mercury crystals. The method being tried first requires that a sample be driven by a quartz

piezoelectric crystal. Up to now we have been unsuccessful in obtaining data. The reason for our lack of success is the difficulty in obtaining a good adhesive to bond mecury to quartz. We have had some success in solving the problem, and it is hoped that the difficulty can be overcome. If not, a torsion pendulum technique, which does not require bonding to the mercury, will be employed.

D. Low Temperature Creep of Mercury

A. Arko
Ph. D. Thesis Research

Since March 1, 1961, this project has been supported by an Air Force Office of Scientific Research contract which became effective at that time.

The progress made on the project prior to this date was, partly with University funds, the construction of a torsional creep apparatus suitable for testing metal specimens at temperatures down to liquid helium temperatures. Under AFOSR support, measurements are in progress.

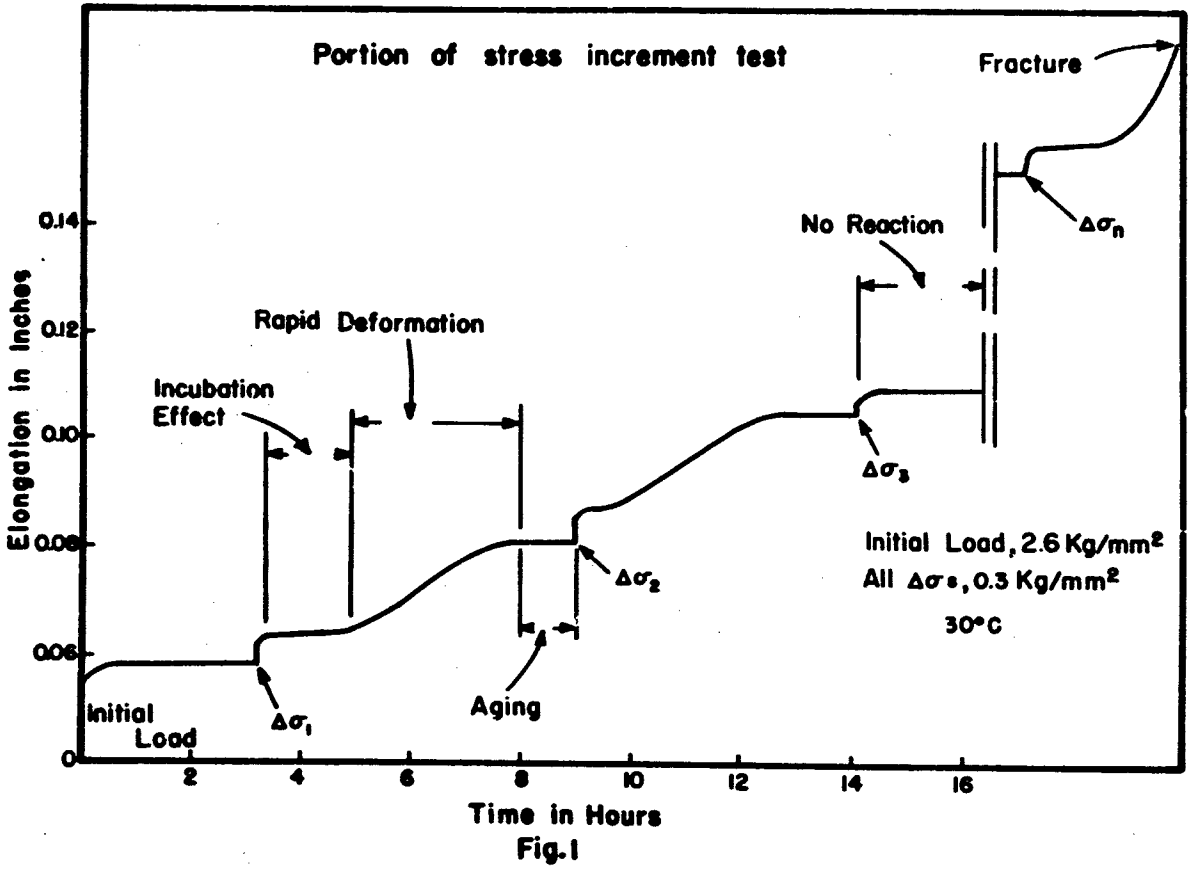
Portion of stress increment test
Fracture
No Reaction
$\Delta\sigma_n$
Rapid Deformation
Incubation Effect
$\Delta\sigma_3$
$\Delta\sigma_2$
Initial Load, 2.6 Kg/mm²
All $\Delta\sigma$s, 0.3 Kg/mm²
30°C
Aging
$\Delta\sigma_1$
Initial Load
Elongation in Inches
0.14
0.12
0.10
0.08
0.06
0
2
4
6
8
10
12
14
16
Time in Hours

Fig.1

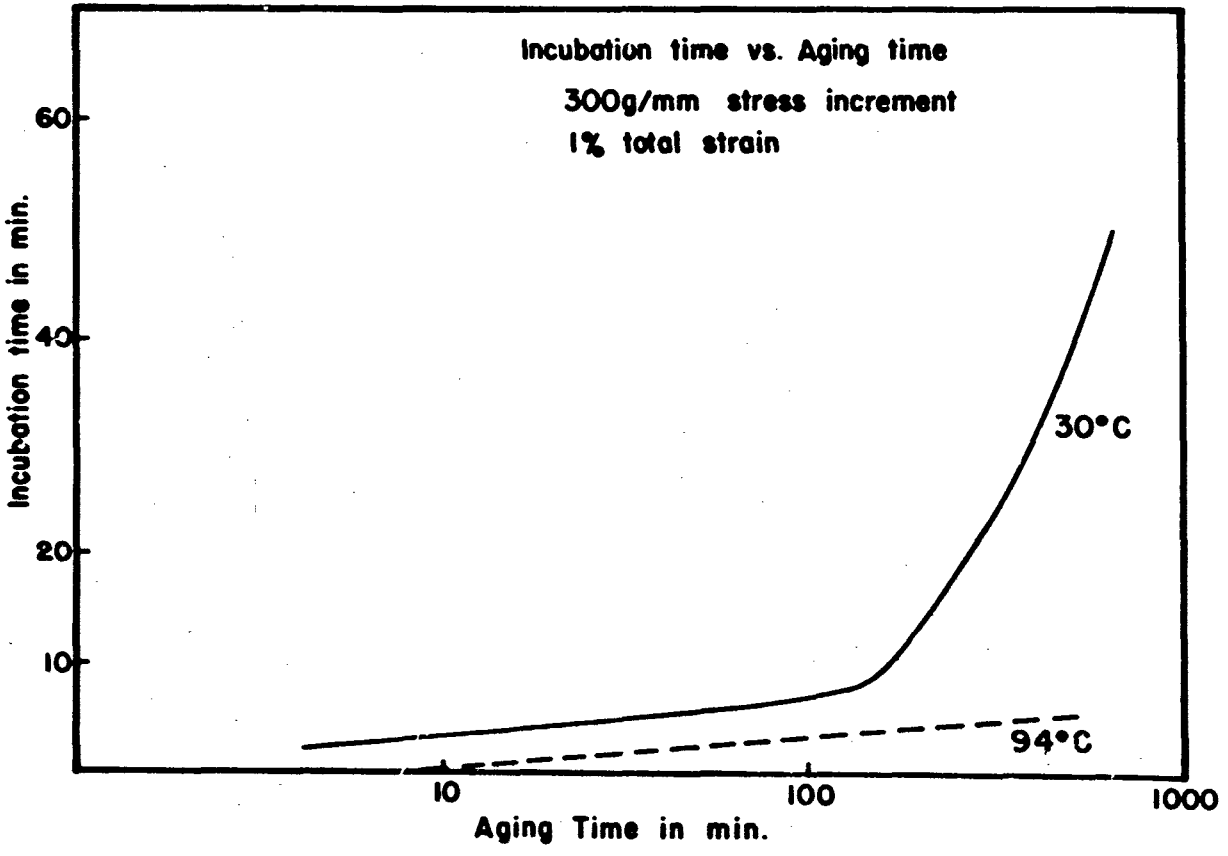
Incubation time vs. Aging time
300g/mm stress increment
1% total strain
Incubation time in min.
60
40
20
10
30°C
94°C
10
100
1000
Aging Time in min.

Fig. 2

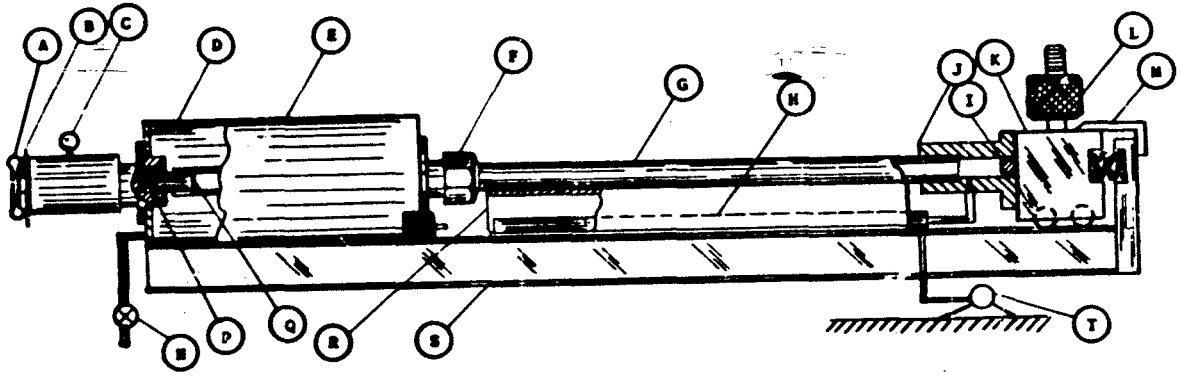

A. Dial Handle
B. Calibrated Dial
C. Trigger
D. Valve
E. Pressure Reservoir
F. Barrel Holder
G. Barrel
H. Vacuum Container
I. Specimen
J. Adapter
K. Specimen Holder
L. C. G. Adjuster
M. Holder Stop
N. Pressure Regulator
O. Striker Holder
P. Striker
Q. Barrel Support
R. Base
S. Vacuum Pump

Fig. 3

Materials Research Project #9

Synthesis, Preparation, and Properties of Compounds Involving I) Ge Double Bonds, II) Si-Transition Metal Bonds

Project Director: A. L. Allred
Assistant Professor, Department of Chemistry

M. Ray
Postdoctoral Research Associate

ABSTRACT

This report discusses: I. Attempts to synthesize A, $[(CH_3)_3C]_2Ge{=}CH{-}CH{=}CH_2$, and B, the heterocyclic compound, 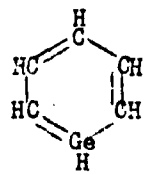 ; and II. The preparation and characterization of compounds containing silicon-transition metal bonds.

Compounds involving pure $p_\pi - p_\pi$ double bonds to elements of atomic number greater than eight probably are heretofore unknown but are expected in projects A and B. While compounds containing carbon-transition metal sigma bonds are relatively few and unstable, the analogous silicon-transition metal compounds may be stabilized by the transfer of electronic charge from the metal to the vacant d orbitals of silicon. All of these projects are under current investigation and incomplete. Attempted syntheses and results are presented. Finally, future plans are outlined.

SCIENTIFIC RESULTS

A. Attempted Synthesis of $[(CH_3)_3C]_2Ge{=}CH{-}CH{=}CH_2$

Introduction:

In the chemical literature there are numerous reports of unsuccessful attempts to prepare compounds containing pure $p_\pi - p_\pi$ double bonds to elements which are not in the first row of the periodic system. Also, in the older literature several claims of the preparation of these compounds appeared but have not been substantiated. Although one can argue that the non-existence of pure $p_\pi - p_\pi$ double bonds to the higher row elements is either due to large bond distance accompanied by slight overlap of adjacent p orbitals or due to the strength of two sigma bonds compared with one sigma and one pi bond, there is at present no rigorous, theoretical justification for either of these explanations. Perhaps the non-existence of these compounds is due to the failure to work with optimum chemical systems and synthesis routes.

In this research, the >Ge=C< linkage was chosen for investigation in view of the similarity of the chemical and physical properties of carbon and germanium[1] and the great propensity of carbon toward double bond formation. In fact, germanium resembles carbon more than silicon does due to the transition metal contraction[1].

The following synthesis route is being investigated:

$$GeCl_4 + 2\ (CH_3)_3CMgCl \rightarrow [(CH_3)_3C]_2GeCl_2 + 2\ MgCl_2$$

$$[(CH_3)_3C]_2GeCl_2 + CH_2{=}CH{-}CH_2MgCl \rightarrow [(CH_3)_3C]_2GeCH_2{-}CH{=}CH_2 + MgCl_2$$

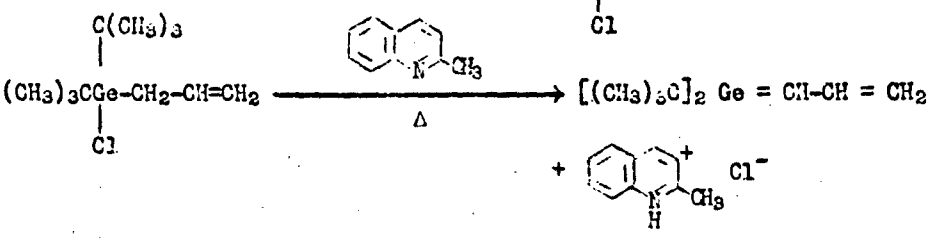

The elimination of the elements of hydrogen chloride and the formation of the double bond in the last reaction should be facilitated by the highly branched tertiary butyl groups, by the electron attracting tendency of the sp^2 -hybridized carbon atoms of the allyl group, by a low polarity solvent, and by high temperature. Also, the combination of bulky groups on germanium and a hindered base make substitution on the germanium by the base unlikely. Finally, the product would be stabilized by conjugation of double bonds. For a general discussion of factors which favor elimination over substitution reactions, see reference 2.

Heretofore no t-butyl derivative of germanium has been reported. In the preparation[3] of t-butyl derivatives of silicon, the second t-butyl group was substituted with difficulty. Refluxing t-butyl-silicon trichloride with t-butyl lithium for four days gave a small yield of di-t-butylsilicon dichloride. Since molecular models indicated that di-t-butylgermanium dichloride is not sterically hindered, conditions for the alkylation of germanium tetrachloride with t-butylmagnesium chloride were investigated.

Experimental:

In a preliminary experiment germanium tetrachloride and t-butylmagnesium chloride were reacted in the molar ratio of 1:2. The t-butyl Grignard reagent was prepared according to the procedure described by Gilman and co-workers[4], and the yield was estimated by titration to be 70 per cent. The reaction mixture was hydrolyzed with caustic soda and extracted with hot carbon tetrachloride. After distilling off the solvent, the residue was digested with concentrated hydrochloric acid, extracted with petroleum ether and fractionated under atmospheric pressure (746 mm). After removal of the petroleum ether, the next fraction distilled over at 165°-166°.

This material condensed to a white solid mass on the cooler parts of the distillation apparatus, was dissolved in petroleum ether, and recrystallized by slow evaporation of the solvent under reduced pressure. The crystalline solid analyzed for $(CH_3)_3CGeCl_3$. Found: C 20.37; H 3.66; Cl 44.24; Calc: C 20.34; H 3.84; Cl 45.07. No di-t-butyl germanium compound was obtained from this experiment.

The new compound, $(CH_3)_3CGeCl_3$, exhibited several unexpected properties. Unlike other known alkyltrichlorogermanes including even those of high molecular weight, it is a crystalline solid which slowly sublimes at room temperature. It does not fume in moist air and has only a faint acrid odor.

In the second attempted synthesis of di-t-butyl germanium dichloride, n-butyl ether was employed as the solvent in order to achieve higher reflux temperature, and germanium tetrachloride and t-butyl Grignard reagent were reacted in the molar ratio of 1:6. Fractionation of the reaction products yielded a small amount of distillate (ca.2 g.;b.p. 90°, 746 mm) which analyzed as $[(CH_3)_3C]_2\ GeCl_2$. Found: C 35.01; H 6.29; Calc: C 37.27; H 7.04.

The formation of t-butyl Grignard was apparently slower in n-butyl ether than in ethyl ether. So in another run t-butyl was prepared using ethyl ether as the solvent, and the next step of the synthesis, i.e. reaction with germanium tetrachloride, was carried out in n-butyl ether. The reaction mixture was evaporated to dryness under reduced pressure, digested with caustic soda to hydrolyze organogermanium halides and finally extracted with carbon tetrachloride. The extract, after distilling off solvent under atmospheric pressure, was fractionated twice under reduced pressure (9 mm). The distillate, collected at 118° - 120°, was found to have the percentage composition, C 45.66; H 8.19, which corresponds approximately to that calculated for $[C(CH_3)_3]_2GeO$, (C,47.39; H,8.94).

It appears that bis-t-butylgermanium oxide exists in more than one modification, especially since compounds of this type tend to form cyclic oligomers easily. Attempts are now being made to prepare this compound in a pure state and in better yield. A determination of molecular weight and other studies of chemical and physical properties are proposed.

The new compound, t-butylgermanoic anhydride, $[(CH_3)_3CGeO]_2O$, was prepared by hydrolyzing $(CH_3)_3CGeCl_3$ with caustic soda, extracting with carbon tetrachloride, and evaporating the solvent. Analysis. Found: C 30.75, 31.12; H 5.35, 5.64; Calc. C 31.25; H 5.86. It forms a white crystalline mass melting at 322 - 325°C. Unlike other alkylgermanoic anhydrides, it is insoluble in water and alkali.

Several unsuccessful attempts have been made to alkylate germanium tetrachloride and t-butylgermanium trichloride with t-butyllithium which is expected to facilitate the substitution of the second t-butyl group because of less steric hindrance.

In summary, (1) the new compounds $(CH_3)_3CGeCl_3$, $[(CH_3)_3CGeO]_2O$, $[(CH_3)_3C]_2GeCl_2$, $[(CH_3)_3C]_2GeO$ were prepared; and (2) the reaction of germanium tetrachloride and t-butylmagnesium chloride in ethyl ether gave $(CH_3)_3CGeCl_3$ and in n-butyl ether gave $[(CH_3)_3C]_2GeCl_2$.

9. Attempted Synthesis of 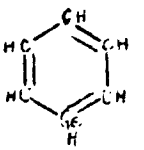

Introduction:

As in Part A, the desired compound contains the $>Ge = C<$ linkage. Two preparative routes were investigated:

1) $HOOC-CH(OH)-CH_2-COOH \longrightarrow$ 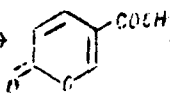 $\longrightarrow HOOC-CH = CH-CH_2-COOH$

1. $LiAlH_4$
2. $SOCl_2$
3. Mg

$ClMg-CH_2-CH = CH-CH_2-CH_2-MgCl$

1. $GeCl_4$
2. $LiAlH_4$

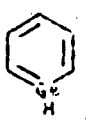

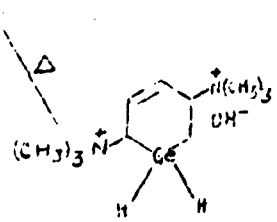

1. 2 N-bromosuccinimide
2. 2 $(CH_3)_3N$
3. Ag_2O

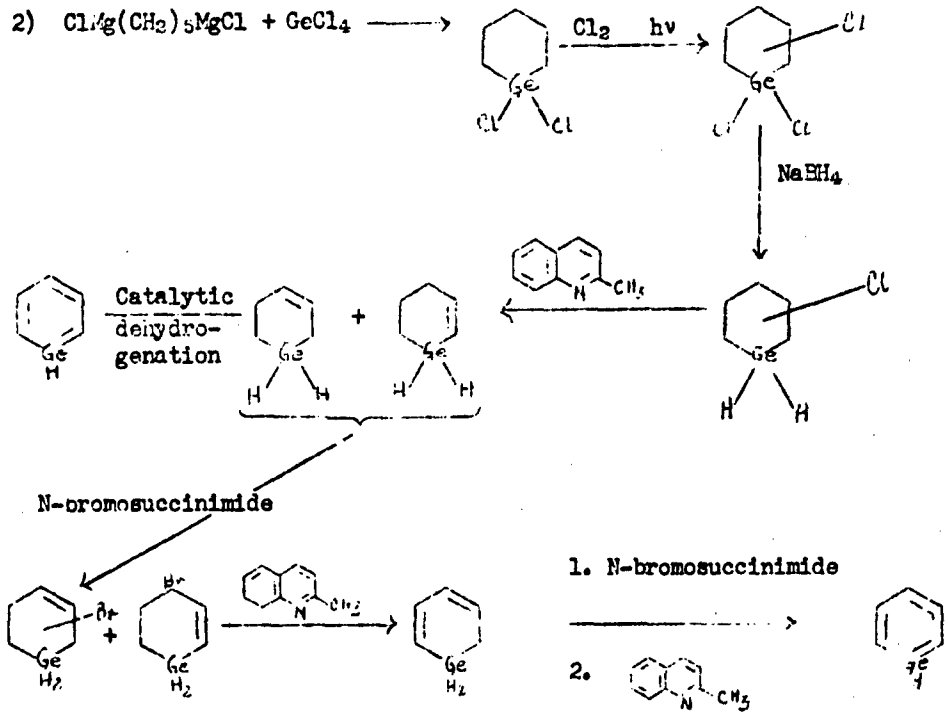

In both of these syntheses, the final step involves a partially unsaturated reactant forming an aromatic compound probably with considerable resonance stabilization. Analogous reactions in organic chemistry are extremely common.

Experimental:

Since the unsaturated dihalide, to be used as the starting material for the first route, is not commercially available or even described in literature, it was necessary to evolve some method to synthesize it. One of the plausible routes is outlined below.

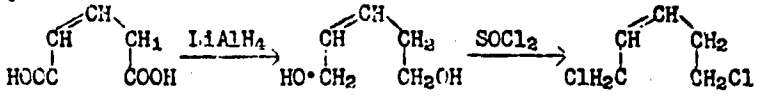

Glutaconic acid

Several methods for the large-scale preparation of glutaconic acid have been described:

1) $HOOC-CH_2-C(OH)(COOH)-CH_2-COOH$ (Citric acid) $\xrightarrow{\text{fuming } H_2SO_4}$ $HOOC-CH_2-CO-CH_2-COOH$ (Acetone-dicarboxylic acid) $\xrightarrow{H_2 - Pt}$ $HOOC-CH_2-CH(OH)-CH_2-COOH$ (β-Hydroxyglutaric acid) $\xrightarrow{\text{Dehydration}}$ Glutaconic acid

2) $CH_2(COOH)-CH(OH)-COOH$ (Malic acid) $\xrightarrow{SO_3\text{-conc.}H_2SO_4}$ Coumalic acid $\xrightarrow[\Delta]{Ba(OH)_2}$ Glutaconic acid (Ref.6)

3) $CH_2Cl-CH(OH)-CH_2Cl$ (α-Dichlorohydrin) $\xrightarrow[\text{in aq. methanol}]{KCN}$ $CH_2CN-CH(CH)-CH_2CN$ $\xrightarrow[H_2SO_4]{EtOH-}$ $CH_2COOEt-CH(OH)-CH_2COOEt$ (Ref.7)

Dissolved in pyridine and treated with Sodium (Ref.8)

$CH_2COOEt-CH-CHCOOEt$ $\xrightarrow{[H_2O]}$ Glutaconic acid

4) $HC\equiv C-COOH$ (Propiolic acid) $\xrightarrow{\text{Alkali metal or alkaline earth metal hydroxide or a quaternary ammonium hydroxide in nitrogen atmosphere}}$ Glutaconic acid (Norman D. Scott to E. I. DuPont de Nemours and Co., U.S. Patent 2,218,032)

The preparation of acetone-dicarboxylic acid from citric acid and its catalytic reduction to β-hydroxyglutaric acid are laborious operations when conducted on a large scale. An alternative method of synthesis[9] which starts with ethyl malonate is extremely slow with a small yield. The synthesis starting with α-dichlorohydrin appears to be more suitable.

The nitrile synthesis has been carried out under a variety of conditions. To a boiling solution of α-dichlorohydrin in methanol under reflux an aqueous solution of potassium cyanide was added. After removing the precipitated potassium chloride, the brown filtrate was evaporated under reduced pressure

at 40° to 50° to yield dicyanohydrin as a brown amorphous residue. Under varied conditions, powdered potassium cyanide was added to a refluxing solution of α-dichlorohydrin in absolute methanol or ethanol in order to obviate the large volume of water needed to dissolve potassium cyanide and thereby to minimize the time required for evaporating the reaction mixture. The formation of nitrile was smooth under all these conditions. The brown residue which consisted essentially of dicyanchydrin was used, without further purification, for the preparation of hydroxyglutaric ester. But the yield of the ester was considerably lower than that reported by Dreifuss and Ingold (loc. cit.).

An unsuccessful attempt was made to convert dicyanohydrin into glutaconic acid according to the method described by Morgenstern and Zerner[10]. The method consisted of refluxing dicyanohydrin with caustic potash and isolating glutaconic acid as its copper salt.

Although coumalic acid was synthesized in fairly good yield from malic acid[11], its conversion into glutaconic acid according to the method described by Pechmann[6] and also with some variations, was not at all satisfactory. The procedure yielded a small amount of light yellow solid which melted around 142° [cf.m.p. of glutaconic acid, 132°-134° (Pechmann); 138° (Dictionary of Organic Compounds.)]

Since no suitable method could be evolved for the synthesis of $ClCH_2CH = CHCH_2CH_2Cl$, it was decided to synthesize the saturated heterocyclic compound of germanium, pentamethylenegermanium dichloride and then introduce double bonds into the ring.

Schwartz and Reinhardt[12] reacted germanium tetrachloride with the double Grignard reagent prepared from 1,5-dibromopentane and fractionated the reaction mixture, after removal of the solvent, under 12 mm pressure. The fraction distilling in the range 55°-60° was found to be the above mentioned heterocyclic compound. The two fractions boiling in the ranges 70°-100° and 100°-200° were not characterized.

We attempted the above synthesis using 1,5-dichloropentane. The two-phase Grignard reagent was slowly added with stirring to germanium tetrachloride, the reaction flask being cooled in ice; the mixture was cooked on a steam-bath, and the precipitated magnesium chloride was filtered off. After removing the solvent, the residual liquid was fractionated under 12 mm pressure. No distillate was obtained in the reported temperature range 55°-60°. Instead, a small amount of liquid distilled over at 71°-76°.

In a different run, several fractions were collected. The temperature ranges in which they distilled over and their analyses are tabluated below.

Fractions	Distilled at (12 mm)	Analysis		
		Carbon	Hydrogen	Chlorine
I	70°	33.84	5.63	28.26 27.76 28.53 28.23
II	94°-98°	56.00	8.50	7.88 7.69 7.69 8.00
III	104°-115°	46.84	7.36	15.13 15.11 15.04 15.04

None of the sets of analytical data check well with the expected heterocyclic compound which should have the percentage composition, C 28.12; H 4.72; Cl 33.24.

Attempts are now being made to achieve a more clear-cut fractionation of the reaction mixture in order to isolate the dichloroheterocyclic compound in pure state and to characterize the other products.

B. Preparation and Characterization of Compounds Containing Silicon-Transition Metal Bonds

Introduction:

The ultimate goal of this project is the preparation of polymers of the type, $\left[\begin{smallmatrix} R \\ | \\ Si-M \\ | \\ R \end{smallmatrix}\right]_x$. At present there are only a few examples of silicon-transition metal bonds and all exist in mixed carbonyl-cyclopentadienyl complex, for example, $C_5H_5Fe(CO)_2Si(CH_3)_3$. Reviews[13,14] of organometallic chemistry discuss the relative scarcity of compounds containing simple, sigma carbon-transition metal bonds. From the array of previously reported carbon-transition metal compounds and from considerations of molecular orbital theory,[14] one can conclude that the stability of sigma bonds between transition metals and carbon or silicon is increased by the addition of appropriate ligands to the metal, is greater for metals with large numbers of d-electrons, and is greater for metals of the second and third transition series than for elements of the first series.

In view of the instability of the alkyl and aryl compounds of the transition metals, polymers of the type, $\left[\begin{matrix} R \\ | \\ C\text{-}M \\ | \\ R \end{matrix}\right]_n$, probably will be unstable. However, analagous polymers of silicon may be stable and exhibit interesting, useful properties for the following reason: Silicon, unlike carbon, has vacant d-orbitals available for bond formation. Thus there exists the possibility of stabilization due to the formation of a double bond due to donation of electrons from filled orbitals of the metal to empty d-orbitals of silicon.

Before attempting the preparation of polymers, it was decided to prepare and characterize a simple transition metal-silicon compound. In view of the above generalizations, the compound chosen for investigation was cis-bis-triethylphosphine-bis-triphenylsilyl-platinum (II). The following reactions were carried out:

1. $PBr_3 + 3CH_3CH_2MgBr \longrightarrow P(CH_2CH_3)_3 + 3MgBr_2$

2. $K_2PtCl_4 + 2P(CH_2CH_3)_3 \longrightarrow 2KCl + [(CH_3CH_2)_3P]_2PtCl_2$

3. $[(CH_3CH_2)_3P]_2PtCl_2 + 2(C_6H_5)_3SiLi \longrightarrow [(CH_3CH_2)_3P]_2Pt[Si(C_6H_5)_3]_2$

Experimental:

Preparation of triethylphosphine: A solution of ethylmagnesium bromide was prepared in 90% yield from the reaction of 48.6 g. (2 g. atoms) magnesium with 218 g. (2 moles) ethyl bromide in 500 mls. of ethyl ether. The Grignard solution was cooled to 0°C. Sixty grams (0.22 mole) phosphorus tribromide dissolved in 200 mls. ethyl ether was added dropwise over a two-hour period to the cooled and stirred Grignard solution. The reaction mixture was refluxed for two hours. Seventy grams of diphenyl ether, b.p. 259°C, was added, the reaction mixture was heated, and triethylphosphine and ethyl ether were distilled, leaving a slurry of magnesium bromide in the diphenyl ether. After redistillation, the yield of triethylphosphine, b.p. 126-127°C, was 90%.

Preparation of cis-bis-triphenylphosphine platinum dichloride: To a solution of 4.15 g. (0.01 mole) of K_2PtCl_4 in 50 ml. of water, 2.4 g. of triethylphosphine was added with stirring. A red-brown precipitate of $Pt[(CH_3CH_2)_3P]_4PtCl_4$ formed and was converted to the monomer, $[(CH_3CH_2)_3P]_2PtCl_2$, by heating at 100°C for 10 minutes. The impure product was washed with water, dried at 105°C for 24 hours, extracted with ethyl ether to remove the trans product, and recrystallized from ethanol. The yield of cis-bis-triethylphosphineplatinum dichloride, m.p. 189°C (reported 191°C), was 45%.

Reaction of cis-bis-triethylphosphineplatinum dichloride with triphenylsilyl lithium: Fifteen grams of hexaphenyldisilane and 3 g. of lithium wire cut into small pieces were mixed. Twenty-five mls. of tetrahydrofuran, previously distilled from lithium aluminum hydride, was added and the resulting paste stirred for 10 minutes. An additional 150 ml. of tetrahydrofuran

was added dropwise and stirring continued for 16 hours. The yield of triphenylsilyl lithium was estimated to be almost 100% by titration to a methyl orange endpoint of aliquots with hydrochloric acid.

Part of the solution of triphenylsilyl lithium (36.1 ml, 0.023 moles) was cooled to 0°C. Then 200 ml. of the solution of dry tetrahydrofuran and 0.502 g. of $[(CH_3CH_2)_3P]_2PtCl_2$ were added during a one-hour period. The solution was stirred at room temperature for one hour with no apparent change. After removal of the solvent by vacuum distillation, a brown amorphous solid remained.

Extraction of the solid residue with dry ethyl ether gave a tan solution. After the addition of n-hexane and the removal of most of the ether, a tan, amorphous precipitate formed. Qualitative tests demonstrated the presence of both platinum and silicon in the tan precipitate. Extraction of the above reaction mixture with benzene led to a brown solid which did not give the correct carbon and hydrogen analysis for the desired product. Attempted separations by column chromatography led to a pasty yellow solid which could not be recrystallized. The solid from the reaction mixture did not sublime at low temperatures and decomposed at high temperatures. Efforts are being continued to purify the product of the above reaction by recrystallization.

Future Plans

Research in the previously discussed projects will continue. If the sequence of reactions on page 31 can be completed, several chemical and physical properties of $[(CH_3)_3C]_2Ge{=}CH{-}CH{=}CH_2$ will be investigated. Of particular interest will be the possibility of free radical polymerization and the properties of the new type of polymer which would result. Additional reactions and cleavage reactions of the $>Ge{=}C<$ linkage with several reagents will be studied. The preparative route, outlined at the top of page 34, will be continued in the synthesis of an aromatic compound of germanium. A comparison of the electronic spectra, force constants of $>C{-}H$ and $>Ge{-}H$ bonds, polarizability and aromatic character of

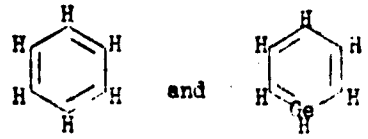

are planned. Before attempting the preparation of polymers containing silicon-transition metal bonds, it is desirable to obtain more information about the reactivity of simple transition metal-silicon compounds. Accordingly, efforts will continue to isolate crystalline $[(CH_3CH_2)_3P]_2Pt[Si(C_6H_5)_3]_2$. Also, in view of the stability of the product of the simple reaction,[25]

$NaMn(CO)_5 + CH_3I \longrightarrow CH_3Mn(CO)_5 + NaI$, the corresponding reaction,

$NaMn(CO)_5 + (CH_3)_3SiI \longrightarrow (CH_3)_3SiMn(CO)_5 + NaI$ will be investigated.

REFERENCES

1. A. L. Allred and E. G. Rochow, J. Inorg. Nucl. Chem., 5, 264, 269 (1958).
2. E. S. Gould, Mechanism and Structure in Organic Chemistry, Chap. 12, Henry Holt and Company, New York (1959).
3. L. J. Tyler, L. H. Sommer, and F. C. Whitmore, J. Amer. Chem. Soc., 70, 2876 (1948).
4. H. Gilman and E. A. Zoellner, J. Amer. Chem. Soc., 53, 1583 (1931).
5. C. K. Ingold and L. C. Nickolls, J. Chem. Soc., 1642 (1922).
6. H. von Pechmann, Annalen der Chemie, 264, 301 (1891).
7. M. H. Dreifuss and C. K. Ingold, J. Chem. Soc., 2964 (1923).
8. B. S. Gidvani, ibid., 2666 (1932).
9. C. K. Ingold and A. E. Perren, ibid., 1414 (1922).
10. O. Morgenstern and E. Zerner, Monatsh., 31, 777 (1910).
11. Organic Syntheses, 31, 23, John Wiley & Sons, New York (1951).
12. R. Schwartz and W. Reinhardt, Ber., 65B, 1743 (1932).
13. F. A. Cotton, Chem. Rev., 55, 551 (1955).
14. H. Zeiss, Organometallic Chemistry, Reinhold, New York (1960).
15. R. D. Closson, J. Kozikowski, and T. H. Coffield, J. Org. Chem., 22, 598 (1957).

Microwave Investigations of Semiconductors and Magnetic Materials

Project Director: M. E. Brodwin
Associate Professor, Department of Electrical Engineering

A. Transport Properties and the Faraday Effect in Semiconductors

J. K. Furdyna
Postdoctoral Research Associate

Previous analyses, based on simple semiconductor models, showed that measurements of the Faraday rotation and ellipticity in semiconductors can be used to determine the conductivity, mobility, static dielectric constant, effective mass, and the collision time. We have carried out a more sophisticated analysis of the problem, based on the Boltzmann transport equation. Our results indicate that the assumptions made in the earlier models are over simplified, especially as regards Faraday ellipticity. The latter phenomenon, apart from its dependence on the parameters enumerated above, is a strong function of the scattering mechanism and of the carrier distribution function. For example, it is found that when the collision frequency exceeds both the cyclotron and the applied frequencies, ellipticity is a strong function of the quantity $\langle\tau^3\rangle/\langle\tau^2\rangle\langle\tau\rangle$, where τ is the energy dependent relaxation time, and the angular brackets denote averages taken with an appropriate distribution function. This quantity is rather sensitive to the type of scattering mechanism, its value ranging from 1.50 for ideal lattice scattering to 3.05 for ionized impurity scattering, as contrasted with the value unity predicted by the constant τ approximation. When either the cyclotron or the applied frequency exceeds the collision frequency, Faraday ellipticity measures directly the quantity $\langle\tau^{-1}\rangle$ rather than $\langle\tau\rangle$. It is also observed that ellipticity can display a sign change, i.e., a reversal in the sense of polarization, as the applied frequency is varied. This feature is attractive to the experimentalist, since the condition for the sign reversal involves few parameters and can be determined with high precision. The preceding analysis indicates that Faraday ellipticity can become a powerful tool in the investigation of these aspects of the transport process.

Some of the above results have been presented at the 1961 Spring meeting of the American Physical Society[1] and a paper has been submitted to the Physical Review[2]. We are presently extending the analysis to specific cases, such as warped surfaces of constant energy and anisotropic relaxation times.

B. Frequency Dependence of Constitutive Parameters in Semiconductors

H. Sherman
M.S. Thesis Research

The simple model of semiconductor behavior at microwave frequencies can be used to predict how the dielectric constant and conductivity should vary as a function of frequency. This aspect of the model has never been experimentally evaluated. It is the object of this investigation to measure these parameters at 3, 1.25, 0.9, and 0.3 cm wavelengths. A preliminary step is the investigation of two new techniques for determining the loss tangent. An interface reflection method for use with lossy and/or thick samples has been studied. The principal feature is that the conductivity or thickness is sufficiently great so that there are no multiple reflections. This method is most useful for lossy materials. A more precise method, employing the Deschamp analysis of two port junctions, requires a sample sufficiently thin to permit significant transmission. The sample completely fills the waveguide and is terminated by an adjustable short circuit. From an analysis of the reflections from the sample as a function of the position of the short circuit, the constitutive parameters can be determined.

Measurements have been made on thin samples by the Deschamp method. Samples of heavily doped germanium were prepared with a thickness of 5-10 mils and measured at 3 cm wavelength. The results agreed reasonably well with estimates of conductivity and dielectric constant.

The present program includes a further evaluation of the two methods and measurements at wavelengths well into the millimeter range.

C. Investigations of Magnetic Materials

D. Miller
Ph. D. Thesis Research

The purpose of this work is the investigation of certain magnetic materials (ferrites and super-paramagnetic materials) by observation of the transmission and standing wave pattern of a coaxial line completely filled with the material under investigation. The attenuation of the material and the wavelength of the wave propagating in the coaxial line will be measured as functions of frequency, static magnetic field intensity, and temperature. The observations will be related to the properties of the materials. In the case of ferrites, the components of the permeability tensor can be obtained. For super-paramagnetic materials, the complex susceptibility will be found.

The experimental investigations are carried out by placing a long sample of the material inside a coaxial line. The coaxial line is placed in a solenoid in order to provide a static magnetic field along the axis of the transmission line. The electric field is probed through a longitudinal slot in the wall of the coaxial line in the vicinity of the sample. A recording is made of the standing wave pattern. Transmission measurements are also made. The frequency is varied in the range of from 500 to 2000 mcs, and the static magnetic field is varied from 0 to 1000 gauss.

The first phase of the investigations on ferrites has been completed. A digital computer solution of the boundary value problem has been carried out and preliminary measurements have been started. To extend the study to higher frequencies it has been necessary to design and construct a new slotted line of much smaller diameter. This instrument has been completed and is undergoing further tests.

The second area, studies of super paramagnetic materials, is presently under way and some preliminary results can be reported. A nickel-nickel oxide material was placed in a 9/16 inch coaxial line and the standing wave pattern was measured at frequencies of 1200 to 2000 mcs in static magnetic fields of from 0 to 1000 gauss. The differential complex susceptibility, g factor, and low frequency spin resonance were observed.

The present program includes an extension of these studies to higher frequencies and various temperatures.

REFERENCES

1. J. K. Furdyna and M.E. Brodwin, "Faraday Ellipticity in Semiconductors as a Function of the Energy-Dependent Relaxation Time", Bull. Am. Phys. Soc., 6, (1961).

2. J. K. Furdyna and M. E. Brodwin "Dependence of the Free-Carrier Faraday Ellipticity in Semiconductors on Scattering Mechanisms," Phys. Rev. (Submitted).

Rheology of Polymers

Project Director: S. Gratch
Associate Professor, Department of Mechanical Engineering

A. Viscoelastic Behavior of Heterogeneous Systems

It has been known for a long time that morphological heterogeneity in general enhances greatly the impact strength of polymer systems[1]. Until now this phenomenon has been attributed to the presence of a discontinuous phase of soft (rubbery) polymer imbedded in a continuous matrix of hard (glassy) polymer.

A quantitative viscoelastic analysis of an idealized model corresponding to this morphology has been carried out. The essential simplifications of this model consist of the assumptions that the rubbery component is distributed in the form of spheres of equal size and that its moduli are much smaller than those of the glassy component. The only other assumption made is that the changes in the stress field in the immediate vicinity of any one sphere which are caused by all the other spheres could be replaced by an equivalent average spherically symmetrical distribution. The results of the analysis showed that the impact strength of such a system actually should be less than that of the homogeneous glassy component alone unless the amount of rubbery phase were so large that buckling of the glassy partitions separating the rubbery spheres could occur before the ultimate strength of the glassy component were reached. For typical polymeric systems this would require an amount of rubbery component in excess of 60% by volume.

Since the literature shows many instances in which high impact strength heterogeneous polymers have been produced with as little as 30% by volume of soft component, it is necessary to postulate a different morphology. In some cases lack of randomness in the distribution of phases may be responsible for the unexpected high impact strength. However investigation by phase contrast microscopy, as well as other evidence, suggests that in many cases the high impact strength polymers consist of a discontinuous hard phase dispersed in a continuous soft matrix which acts as a binder. This alternative model has also been analyzed quantitatively, with results in excellent agreement with the experimental observations reported in the literature. It has been shown that such a morphology is capable of giving the relatively high moduli observed. It has also been shown that such a morphology would give a stress-strain diagram similar in shape to that of ductile metals with pronounced yield points. Such stress-strain diagrams are actually observed with many high impact strength heterogeneous polymers.

B. Thermoviscoelasticity

R. Wolosewic and R. Petrof
M. S. Thesis Research

In the case of classically elastic materials, it has been found that the dynamic behavior (high speed vibrations, impact, etc.) may be affected significantly by the coupling between elastic response and heat transfer[2]. There is nothing at all in the literature on the corresponding effect for viscoelastic materials, even though a priori it would be expected that such a coupling would be particularly important, for instance, for rubber-like high polymers. The reason for this gap in the literature evidently is the extreme complexity of the problem. Dynamic problems are quite complex in the case of viscoelastic materials even under isothermal conditions[3]. The introduction of temperature non-uniformity presents frightful difficulties even when the temperature distribution is prescribed independently of the stress distribution[4]. It is clear, therefore, that the problem of transient stresses in viscoelastic materials when the temperature distribution is coupled with the variation in stresses is one of the greatest magnitude.

So far, as part of this program, this problem has been formulated in two alternative manners, one involving a system of four simultaneous non-linear partial differential equations, another involving an integro-differential equation of Volterra's second kind coupled with three partial differential equations. Efforts are being made to reduce either one of these systems of equations to a form suitable for numerical solution by means of a digital electronic computer.

These researches will be terminated since the principal investigator has left for the Ford Motor Research Laboratory.

REFERENCES

1. e.g. Merz et al., J. Polymer Sci., 22, 325 (1956); Keskkula, J. Appl. Polymer Sci., 2, 289 (1959); Schmitt and Keskkula, J. Appl. Polymer Sci., 3, 132 (1960); Davenport et al., Brit. Plastics, 32, 549 (1959).

2. e.g. Boley and Weiner, "Theory of Thermal Stresses," Wiley, New York, 1960; Sneddon and Hill, ed., "Progress in Solid Mechanics," vol. I., Chapt. VI, Interscience, New York, 1960.

3. Sneddon and Hill, ed., loc. cit., Chapt. I.

4. Muki and Sternberg, J. Appl. Mech., to be published (ASME Paper No. 60-WA-124).

Syntheses and Solid State Reactions of Metal Complexes

Project Director: F. Basolo
Professor, Department of Chemistry

S. K. Dhar
Postdoctoral Research Associate

ABSTRACT

The materials tris (2, 2′ - bipyridine) metal (II) bromides, $[M(bipy)_3]Br_2$, where M = Mn, Fe, Co, Ni, Cu or Zn, have been prepared and characterized by analysis. Their thermal stabilities towards the loss of one or two 2, 2′ - bipyridine groups were determined by measurements of weight loss as a function of temperature. This was done by using a thermogravimetric balance. It has not yet been possible to obtain sufficiently good data to permit reliable estimates of rate constants and activation energies for these processes.

INTRODUCTION

The primary purpose of this research is to investigate the thermal stability and solid state reactions of metal complexes. These materials contain a central metal atom or ion surrounded by a cluster of ions or molecules. It is characteristic of the complex that it retains its identity even in solution, except for possibly some dissociation. The complex may be an anion, non-ionic or a cation depending on the charges carried by the central atom and the coordinated groups. These groups are called ligands, and the total number of attachments to the central atom is called coordination number. For example the compound $K_2[PtCl_6]$ contains chloro ligands and the platinum(IV) is said to have a coordination number of six. A non-ionic complex may be illustrated by $[Co(NH_3)_3(NO_2)_3]$ and a cationic one by $[Ni(NH_2CH_2CH_2NH_2)_3]SO_4$.

The reaction processes of these materials in solution have been investigated in some detail (Basolo and Pearson, Mechanisms of Inorganic Reactions, John Wiley and Sons, New York, 1958). However very little is known about their reactions in the solid state. Yet reactions of this type are known to occur and it is desirable to learn more about them. The reason that no such systematic studies on these materials have been made previously is perhaps due to the many difficulties encountered with quantitative investigations of reactions in the solid state. Now with the availability of thermogravimetric and differential thermal analysis techniques, it should be possible to obtain some useful information on certain of these systems.

The results of this research should increase our knowledge of how metal complexes react in the solid state. It will provide information as to the thermal stability of these materials and may help us design

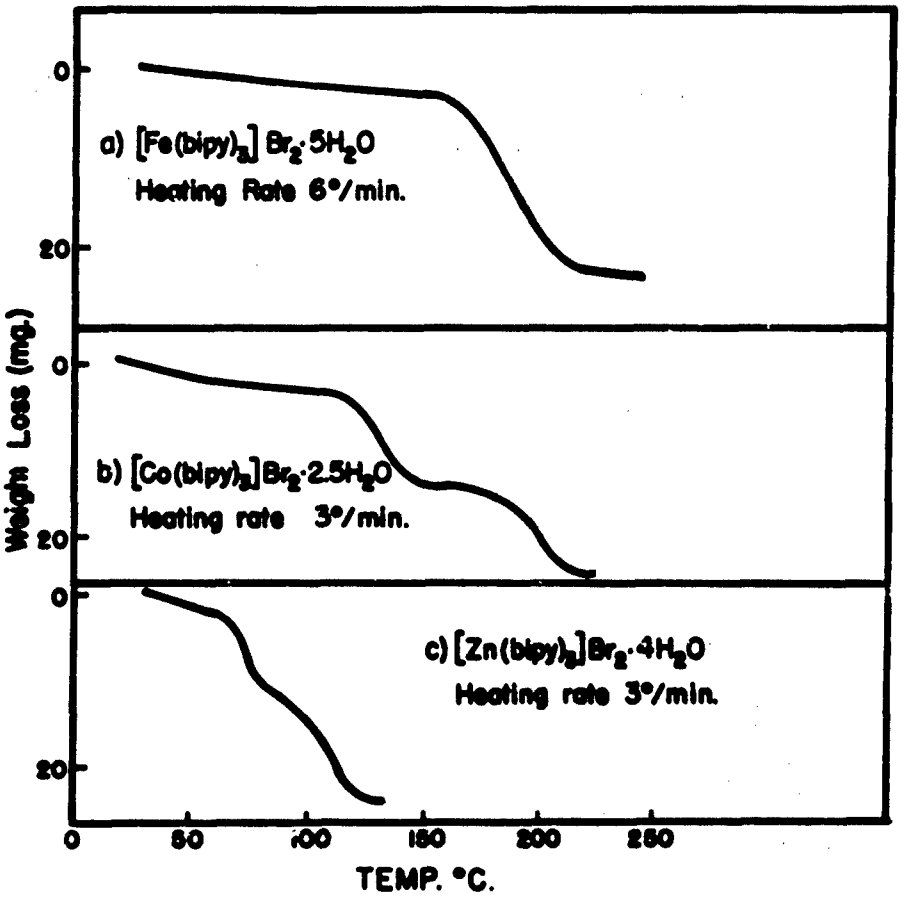

Fig. 1—Sample Thermograms

other methods of synthesis of known or of new compounds. It is also hoped that what we learn will apply in a more fundamental way to solid state reactions in general.

The specific reactions under investigation are

$$[M(bipy)_3]\,X_2 \xrightarrow[-\ bipy]{\Delta} [M(bipy)_2\,X_2] \xrightarrow[-\ bipy]{\Delta} [M(bipy)\,X_2]$$

where M(II) = first row transition metals, X^- = Cl^-, Br^- and I^-, and bipy = 2,2′ - bipyridine. Lower complexes of iron(II) had been prepared previously by this thermal dissociation process (Basolo and Dwyer, J. Am. Chem. Soc. 76, 1454 (1954)). The progress of these reactions is followed by means of a thermogravimetric balance which records weight loss versus time and temperature. The purpose of this study is to determine the rates and activation energies for the reactions as a function of M(II) and of X^-. From a consideration of the crystal-field theory as applied to metal complexes, it is believed that the activation energies for dissociation will show minima at Mn(II) and Zn(II) as one goes from V(II) through Zn(II) across the first transition series. There is also some qualitative evidence that for the same M(II) the thermal stability will increase in the order $Cl^- < Br^- < I^-$. These are the best guesses as to what is expected to happen, so it is with these views in mind that experimental data are being collected to determine whether or not one finds agreement with current theories.

The following description of the experimental work done to date covers 1) the preparation of materials, 2) determination of thermograms and characterization of thermal products, 3) treatment of data, and 4) present status.

PREPARATION OF MATERIALS

The compounds used in this investigation are known materials and were prepared by methods described in the literature. Analyses are given in Table I and a brief discription of the methods of synthesis follows.

[Mn(bipy)$_3$]Br$_2$. This compound was prepared by a method reported in the literature (Burstall and Nyholm, J. Chem. Soc., 3570 (1952)).

[Fe(bipy)$_3$]Br$_2$·5H$_2$O. This compound was prepared by a modification of the method given for [Fe(bipy)$_3$](ClO$_4$)$_2$ by Burstall and Nyholm, J. Chem. Soc., 3570 (1952)).

[Co(bipy)$_3$]Br$_2$·5H$_2$O. This compound was prepared by a modification of the method given for [Co(bipy)$_3$](ClO$_4$)$_2$ by Burstall and Nyholm (loc. cit).

[Ni(bipy)$_3$]Br$_2$2H$_2$O. The compound was prepared according to the method of Burstall and Nyholm (loc. cit). The elemental analysis of the product corresponds to [Ni(bipy)$_3$]Br$_2$.5H$_2$O instead of the reported [Ni(bipy)$_3$]Br$_2$.6H$_2$O.

[Cu(bipy)$_3$]Br$_2$.H$_2$O. This compound was prepared by a modification of the method given for [Cu(bipy)$_3$]SO$_4$.7H$_2$O in the literature (Z. Anorg. Allgem. Chem., 227, 278, (1938)).

[Zn(bipy)$_3$]Br$_2$.4H$_2$O. The compound has been prepared by a modification of the method given for [Zn(bipy)$_3$]SO$_4$.7H$_2$O in the literature (Z. Anorg. Allgem. Chem., 227, 278, (1938)).

TABLE I

ANALYSIS OF THE TRIS (2,2'-BIPYRIDINE)METAL(II) BROMIDES

Compound	Calculated %			Observed %		
	C	H	N	C	H	N
[Mn(bipy)$_3$]Br$_2$	52.4	3.52	12.4	52.5	3.33	12.4
[Fe(bipy)$_3$]Br$_2$.5H$_2$O	46.6	4.4	10.8	46.5	4.6	10.9
[Co(bipy)$_3$]Br$_2$.2.5H$_2$O	49.2	3.96	11.4	49.4	4.14	11.24
[Ni(bipy)$_3$]Br$_2$.5H$_2$O	46.5	4.38	10.8	46.8	4.50	11.0
[Cu(bipy)$_3$]Br$_2$.H$_2$O	50.6	3.66	11.8	50.3	3.58	12.1
[Zn(bipy)$_3$]Br$_2$.4H$_2$O	47.2	4.13	10.9	47.3	4.30	10.9

DETERMINATION OF THERMOGRAMS AND CHARACTERIZATION OF THERMAL PRODUCTS

The thermogravimetric balance used for these determinations is an instrument manufactured by the American Instrument Company. It consists of a spring balance with a transducer assembly, a glass suspension rod and crucible holder. The crucible holder is housed in a furnace tube. For the present investigation a heating rate of 3°C/min has been used. Sample thermograms are shown in Fig. 1. Data collected on these systems are summarized in Table II and analyses of the thermal products are given in Table III . Specific remarks on entries in Table II follow.

[Mn(bipy)$_3$]Br$_2$. With a finely powdered sample, the thermogram consists of 2 steps with a weight loss ratio for step 1: step 2 of ca 0.9:1. A coarsely powdered sample reduces the ratio to ca 0.6:1. This behavior shows the pronounced effect of particle size. A part of the sample above a minimum particle size appears to escape dissociation in its correct temperature range. The theoretical ratio of 1:1 could probably be attained with more effective grinding.

$[Fe(bipy)_3]Br_2 \cdot 4H_2O$. The thermogram (Fig. 1a) indicates a preliminary partial elimination of H_2O, followed by the main break. The significance of the two inflections on the main break is not yet clear. The final product is $[Fe(bipy)]Br_2$.

$[Co(bipy)_3]Br_2 \cdot 2.5\ H_2O$. The thermogram (Fig. 1b) indicates a preliminary loss of 2.5 H_2O followed by the loss of 1 bipy to give $Co(bipy)_2Br_2$. Elemental analysis of the product corresponding to the plateau after the second step indicates the composition $Co(bipy)_{1.5}Br_2$ (Table II). According to the thermogram, however, the weight loss due to the second step is larger than 0.5 equivalents of bipy. A partial sublimation of the complex could account for this discrepancy.

$[Ni(bipy)_3]Br_2 \cdot 5H_2O$. The thermogram indicates an initial partial elimination of H_2O followed by a major break indicating coelimination of the rest of the water and approximately 1.5 equivalents of bipy. Particle size is also markedly important in this process.

$[Cu(bipy)_3]Br_2 \cdot H_2O$. Because of the early issociation of the copper complex (Table I) the particle size plays a role here similar to that with the manganese compound, though somewhat less pronounced in magnitude. Thus effective grinding is important.

$[Zn(bipy)_3]Br_2 \cdot 4H_2O$. The thermogram (Fig. 1c) indicates an initial partial elimination of water, with the rest of the water and 2 bipy eliminated in the main break. The cause of the inflection at ~92°C is not yet clear and further investigation is necessary to elucidate this observation.

All the samples were carefully ground in the same way as was the manganese compound. Except for the approximate compositions $Ni(bipy)_{1.5}Br_2$, and $Co(bipy)_{1.5}Br_2$, the end products of the dissociation steps for the series correspond to $M(bipy)Br_2$ with the intermediate formation of $M(bipy)_2Br_2$ in the case of Mn^{2+} and Cu^{2+}. The nature of $M(bipy)_{1.5}Br_2$ for Co^{2+} and Ni^{2+} has yet to be elucidated. The Ni^{2+} and Fe^{2+} compounds also demonstrate strikingly the effect of the outside anion on the thermal stability of these compounds. Stable intermediates of $Ni(bipy)_2Cl_2$ and $Fe(bipy)_2Cl_2$ are reported but in contrast to this is the apparent thermal instability of the analogous bromides.

TREATMENT OF THE DATA

The energy of activation of a solid state dissociation process may be determined by the application of the familiar Arrhenius expression $k = Ze^{-E^*/RT}$, where Z = frequency factor, E^* = activation energy, and k = rate constant.

If the compound undergoing heating is in a state of dynamic equilibrium, each point slope on the thermogram yields the corresponding rate of reaction at the particular temperature. Thus one should be able to obtain a series of such data from a thermogram which would permit determination of the activation energy from a single experiment.

Freeman and Carroll [J. Phys. Chem. 62, 394, (1958)] have given a simplified graphical treatment. This treatment has been tried in some detail by us and been found to suffer from considerable limitations. Values of E* corresponding to the reaction $CaC_2O_4 \cdot H_2O \triangleq CaC_2O_4 + H_2O$ (in vacuo) fluctuated in the range of 18 - 26 KCal mole^{-1} and values for the reaction $[Mn(bipy)_3]Br_2 \triangleq Mn(bipy)_2 Br_2 + bipy$ (in vacuo) fluctuated in the range of 12 - 18 KCal.

A second approach was tried by assuming the reaction to be first order and determining the reaction rate constant k from the following relation: $\frac{dx}{dt} = k(a-x)$, where a = initial concentration of the tris compound and x is the concentration at time t. Application of this equation presupposes a precise knowledge of the dissociation reaction. The activation energy values determined by this method were equally inconsistent.

In a third approach the dissociation process $CaC_2O_4 \cdot H_2O \triangleq CaC_2O_4 + H_2O$ was studied isothermally. The same trend of fluctuations in the data was observed.

More work is in progress to investigate the cause of this irreproducible behavior. Some thermogravimetric data on the dissociation reaction $CaC_2O_4 \cdot H_2O \triangleq CaC_2O_4 + H_2O$ are being obtained from the Argonne National Laboratory to ascertain if our difficulty is due to instrumental defect. More attention is being paid to the physical parameters which seem to significantly control the course of TGA data as evidenced from recent reports. Solution of this problem precedes any further quantitative study.

PRESENT STATUS

The solid state thermal dissociation of the series of compounds represented by $[M(bipy)_3]Br_2 \cdot XH_2O$ (M^{2+} = first row transition series elements in dipositive oxidation states) may be given by the following expected schematic:

$$[M(bipy)_3]Br_2 \cdot XH_2O \triangleq [M(bipy)_2]Br_2 \cdot (X-y)H_2O + bipy + yH_2O$$

$$[M(bipy)_2]Br_2 \cdot (X-y)H_2O \triangleq [M(bipy)Br_2] + bipy + (X-y)H_2O$$

The experiments are conducted in a vacuum of 400-500 microns under which condition the free bipyridyl groups sublime away from the reaction product. The water molecules set free in the heating process also vaporize in vacuo. The loss in weight thus caused by the physical elimination of a part of the reaction product makes possible the use of the thermogravimetric technique in the study of the above stated thermal dissociation process.

By using a recording thermogravimetric balance with a linear rate of heating it should therefore be possible to follow the kinetics of the process and determine the energy of activation of the various steps. A comparison of the activation energies of the dissociation steps for these compounds is expected to be more meaningful than merely comparing their decomposition temperatures.

The thermogravimetric approach, however, suffers from a number of limitations. While the overall shape is fairly reproducible, the thermograms vary in their details and fail to yield satisfactorily reproducible activation energy data on a critical treatment. The main factors contributing to the difficulties are discussed below.

1) Unlike the case of a reaction in solution, the kinetics of a solid state reaction is dependent on factors such as rates of nucleation and propagation, and the desorption and diffusion of reaction products out of the system. In many cases the solid state dissociation process takes place through an initial induction phase which is known to be largely irreproducible. Pulverizing the sample to a sufficiently small size is important both to ensure complete reaction and to reduce this induction period. Unfortunately the bipyridyl complexes being studied in this investigation are "soft" and do not easily lend themselves to fine grinding by conventional means.

2) Since the observed kinetics depends upon the rate of diffusion of the volatile reaction product out of the system, the "packing" of the sample in the sample holder also appears to be an important parameter.

3) The recorded sample temperature is the temperature in the neighborhood of the crucible holding the sample and is not necessarily the same as that of the actual sample.

4) The bipyridine produced as a reaction product sublimes under vacuum. Since only a part of the suspension system is inside the furnace tube there remains the possibility of the partial condensation of bipy on the suspension system and resublimation on its way out of the assembly. In addition the decomposition products in some cases have been observed to be volatile at high temperature. These then condense on the cooler part of the furnace tube and the suspension rod. The data in such cases are obviously unacceptable.

5) All the bipyridyl complexes studied so far except $[Mn(bipy)_3]Br_2$ are associated with water molecules held in the crystal lattice. In the case of Fe^{2+}, Ni^{2+}, Co^{2+}, and Zn^{2+} the thermograms indicate coelimination of water and bipyridyl. This circumstance contributes to the lack of knowledge of the precise mode of dissociation of these complexes.

Notwithstanding the above factors, which, unless they are properly taken into account, will invalidate much of the quantitative data, it is hoped that the relative errors in a series such as the one under investigation will be similar and thus will not markedly affect the comparative study.

FUTURE INVESTIGATIONS

For the immediate future we will continue our studies of the $[M(bipy)_3]X_2$ systems. It is imperative that we resolve the present difficulty of being unable to obtain reproducible quantitative results. When this problem has been overcome it still remains necessary to attempt to differentiate between the loss of water and loss of bipy. This may require the synthesis of the anhydrous salts. Finally it will then be necessary to prepare and study the V(II) and Cr(II) complexes. These materials have been purposely put off until last as they are difficult to prepare because of the sensitive nature of the metals in this low oxidation state.

Other systems which show promise for studies of this type are illustrated by the following

$$[M(NH_3)_5H_2O]\ X_3 \triangleq [M(NH_3)_5X]\ X_2 + H_2O$$

M(III) = Co(III), Rh(III), Ir(III), Cr(III)

X^- = halides, NCS^-, NO_2^-, SO_4^{2-}, CO_3^{2-} (1)

$$[Cr(en)_3]\ X_3 \triangleq [Cr(en)_2X_2]\ X + en$$

en = $NH_2CH_2CH_2NH_2$

X^- = Cl^- product is Cis; NCS^- product is trans (2)

$$\text{trans} - [Cr(en)_2Cl_2] \triangleq \text{Cis} - [Cr(en)_2Cl_2] \quad (3)$$

$$[(NH_3)_5M\text{-}ONO]\ X_2 \triangleq [(NH_3)_5M\text{-}NO_2]X_2$$

M(III) = Co(III), Rh(III), Ir(III) (4)

$$d - K_3[Cr(C_2O_4)_3] \triangleq d, l - K_3[Cr(C_2O_4)_3] \quad (5)$$

Ni(II) (Schiff base)$_2$ $\triangleq$ Ni(II) (Schiff base)$_2$
(diamagnetic) (paramagnetic) (6)

TABLE II

SCHEMATIC OF THERMAL DISSOCIATION OF THE BIPYRIDYL COMPLEXES

Compound	First Step Temp. range	Wt. loss	Second Step Temp. range	Wt. Loss	Total Wt. Loss
$[Mn(bipy)_3]Br_2$	40° - 75°,	~ 1 bipy	158° - 195°,	1 bipy	~ 2 bipy
$[Fe(bipy)_3]Br_2.5H_2O$	162° - 215°,	2 bipy + nH_2O	Sublimation of Complex		2 bipy + $5H_2O$
$[Co(bipy)_3]Br_2.2.5H_2O$	120° - 153°,	1 bipy	170° - 218° (+ Sublimation of Complex	½ bipy	$1\frac{1}{2}$ bipy + $2.5H_2O$
$[Ni(bipy)_3]Br_2.5H_2O$	188° - 232°,	$1\frac{1}{2}$ bipy + nH_2O	Sublimation of Complex		~ $1\frac{1}{2}$ bipy + $5H_2O$
$[Cu(bipy)_3]Br_2.H_2O$	39° - 84°,	1 bipy + H_2O	1 bipy		2 bipy + H_2O
$[Zn(bipy)_3]Br_2.4H_2O$	65° - 121°,	2 bipy + nH_2O	———		2 bipy + $4H_2O$

TABLE III

ANALYSES OF THERMAL PRODUCTS

Compound	Calculated %			Observed %		
	C	H	N	C	H	N
$Mn(bipy)Br_2$	32.4	2.15	7.58	33.3	2.22	7.76
$Fe(bipy)Br_2$	32.4	2.14	7.54	32.6	2.19	7.47
$Co(bipy)_2Br_2$	45.2	3.07	10.5	45.7	2.99	10.3
$Co(bipy)_{1.5}Br_2$	39.4	2.63	9.2	40.4	2.73	9.3
$Ni(bipy)_{1.5}Br_2$	39.8	2.66	9.3	38.1	2.65	9.1
$Cu(bipy)_2Br_2$	44.9	2.98	10.5	44.0	3.22	10.9
$Cu(bipy)Br_2$	31.6	2.11	7.29	31.6	2.15	7.56
$Zn(bipy)Br_2$	31.5	2.10	7.34	31.5	2.09	7.50

Effect of Structure on the Strength Properties of Clays

Project Director: J. O. Osterberg
Professor, Department of Civil Engineering

W. Perloff, Jr.
Ph.D. Thesis Research

A. Particle Orientation and Reorientation

Indirect evidence from macroscopic soil behavior has indicated that changes in particle orientation and spacing may be causative factors in the variations of pore water pressure and strength which result from changes in the rate of strain and in the stress history. Direct evidence to this effect is lacking at the moment. However, attempts have been made to measure particle orientation by means of x-ray diffraction. Recent results have shown distinct differences between the patterns from oriented and non-oriented samples. The remainder of this project will be spent in determining directly if a correlation between particle orientation and reorientation, and the factors discussed above, actually exists.

B. Pore Water Pressures

The stresses on, and between, the soil particles in the failure zone at failure can be determined only if the pore water pressure in this zone is known. Pore pressure dissipation tests under constant load, as well as moisture distribution studies made recently by other investigators, indicate that significant pressure gradients exist in the pore water in a sample subjected to shear. It was, therefore, necessary to devise a method of measuring the pressure in the failure zone itself, rather than at the base of the specimen, as is customary. These measurements are accomplished with the aid of a hollow needle - like tube with perforated sides. The tube is filled with a fine copper screen in order to prevent clay from flowing into the openings. It is connected by a flexible tube to a mill-balance type of pressure measuring device, and is filled with air-free distilled water. The tube is inserted into the central portion of the clay specimens before testing. This arrangement permits the direct measurement of pressure in the failure zone.

Results of triaxial compression tests with pore water measurements indicate that the water pressure at failure (and, therefore, the magnitude of the interparticle forces) is a function both of the stress history and of the rate of strain. It has been found possible to express these relationships explicitly for one soil by an equation of the form

$$\frac{\Delta U_f}{\sigma_c} = a\left(\frac{\sigma_p}{\sigma_c}\right)^b + c$$

where ΔU_f is the pore water pressure at failure, σ_c the present consolidation pressure, σ_p is the preconsolidation pressure, and a, b, and c are experimental constants. Efforts are being made to extend the results to include other soils.

FUTURE PLANS

Some of the phases of this work which we hope to carry out in the future are:

1) A study of the effect of the type and concentration of ions in the pore fluid on the relationships between strength, interparticle forces, and rate of strain.

2) A study of the relationship between clay mineral type and the effect of rate of strain on strength and interparticle forces.

Polymer Studies

Project Director: M. Dole
Professor, Department of Chemistry

ABSTRACT

A. Hydrogen-Deuterium Exchange Experiments on Irradiated Polyethylene

M. Dole

Kinetic equations have been developed that describe accurately the exchange of deuterium atoms with hydrogen atoms between the gas phase and solid polyethylene at room temperature subsequent to an irradiation with Co-60 γ-rays at liquid nitrogen temperature. Conclusions reached are that (1) the free radicals decay by a first order process, (2) the exchange probably occurs on nearest neighbor sites, and (3) the reaction rate is about 1000 fold faster than it would be if the reaction occurred entirely in the gas phase. The latter fact is explained on the basis of the heat of adsorption of atomic deuterium in the solid lowering the energy of activation for the reaction.

B. Specific Heat Measurements on Polypropylene

R. W. Wilkinson
Ph.D. Thesis Research
University of London, but done at Northwestern

Specific heat measurements have been made on granular and annealed isotactic polypropylene, and on granular atactic polypropylene, the latter over the temperature range -60 to 200°C. Experiments are in progress on annealed atactic polypropylene.

C. Molecular Hydrogen Back Reaction with Irradiated Polyethylene

A. G. Mueller, Jr.

This research has progressed only to the point of attempting to set up a vacuum line free of leaks.

SCIENTIFIC RESULTS

A. Hydrogen-Deuterium Exchange Experiments on Irradiated Polyethylene

The experimental aspects of the study of the exchange of hydrogen isotopes between gaseous deuterium and irradiated polyethylene have been carried out by Dr. Francis Cracco, who was supported by a grant from the U. S. Atomic Energy Commission. With ARPA support, theoretical

equations for the exchange have been developed. If we assume the kinetic equations

$$-CH_2\dot{C}HCH_2- + D_2 \rightarrow -CH_2CHDCH_2- + D^\bullet \quad (1)$$

$$-CH_2CH_2\dot{C}H_2- + D^\bullet \rightarrow -CH_2\dot{C}HCH_2- + HD \quad (2)$$

$$-CH_2\dot{C}HCH_2- + HD \rightarrow -CH_2CHDCH_2- + H^\bullet \quad (3a)$$

$$\rightarrow -CH_2CH_2CH_2- + D^\bullet \quad (3b)$$

$$-CH_2CH_2\dot{C}H_2- + H^\bullet \rightarrow -CH_2\dot{C}HCH_2- + H_2 \quad (4)$$

and let x, y and z equal the mole fractions of D_2, HD and H_2 in the gaseous phase, t the time in hours, k_1 the reaction rate constant of (1), we find that

$$x = \exp(-at) \quad (5a)$$

$$y = \{a/(a - b)\}\,[\exp(-bt) - \exp(-at)] \quad (5b)$$

$$z = 1 - x - y \quad (5c)$$

where

$$a = \frac{w/V \cdot k_h k_1 [R\cdot]^\circ}{1 + \frac{w}{V} k_h} \quad (6)$$

and

$$b = a \frac{k_{3_a}}{k_1} . \quad (7)$$

In Eq. (6) w is the weight of polyethylene, V is the free gas volume of the exchange cell, k_h is Henry's Law constant and $[R]^\circ$ is the initial concentration of free radicals in the polyethylene at the start of the exchange. However, Eqs. (5a) and (5b) were found to be invalid because of the decay of free radical concentration with time. In case the free radicals disappear according to a second order law (the usual situation),

$$[R\cdot] = [R\cdot]^\circ / \{1 + k_3 [R\cdot]^\circ t\} \quad (8)$$

then Eqs. (5) become

$$x = (1 + Bt)^{-a/B} = \exp\left\{-\frac{a}{B} \ln(1 + Bt)\right\} \quad (9a)$$

$$y = [a/(a - b)]\,[\exp\{-\frac{b}{B} \ln(1 + Bt)\} - \exp\{-\frac{a}{B} \ln(1 + Bt)\}] \quad (9b)$$

where

$$B = k_3 [R\cdot]^\circ \quad (10)$$

But Eqs. (9) also do not agree with the data although they are more nearly valid than Eqs. (5). Therefore, a first order free radical decay

$$[R\cdot] = [R\cdot]^{o} \cdot q \tag{11}$$

where

$$q = \exp\{-k_3 \tau\} \tag{12}$$

was tried. The resulting equations are

$$x = \exp\left[-\frac{a}{k_3}(1 - q)\right] \tag{13a}$$

$$y = a/(a - b)\left[\exp\left\{-\frac{b}{k_3}(1 - q)\right\} - \exp\left\{-\frac{a}{k_3}(1 - q)\right\}\right] \tag{13b}$$

these equations give a good description of the data. In addition to Eqs. (13) we also have: at very short times (for all three mechanisms)

$$y = at \tag{14}$$

$$K' = y^2/x.z = 2a/b \tag{15}$$

For Eq. (13) only, at infinite time

$$\ln x_{\infty} = -a/k_3 \tag{16}$$

Equations (14), (15), and (16) permit the evaluation of the constants a, b and k_3. Knowing $[R]^{o}$ from published data and k_h from unpublished results of this laboratory, we can also calculate k_1. It is concluded that reaction (1) proceeds about 1000-fold faster in the solid polyethylene than in the gas phase. This surprising result is attributed to a possible large heat of adsorption of atomic deuterium on the solid polyethylene which reduced the activation energy of (1) sufficiently to account for the greatly enhanced reaction rate.

B. Specific Heat of Isotactic and Atactic Polypropylene

Partially supported by Esso Research and Development Company

The complete results of the specific heat measurements of isotactic polypropylene are given in Table I.

TABLE I

SPECIFIC HEATS OF ISOTACTIC POLYPROPYLENE

(cal/g°C)

Granular		Annealed	
t°C. Ave.	c_p	t°C. Ave.	c_p
-14.361	0.3284	-13.891	0.3408
- 7.916	0.3488	- 1.326	0.3783
- 0.615	0.3687	13.173	0.4014
10.188	0.3882	27.322	0.4361
24.609	0.4279	40.899	0.4657
35.392	0.4603	54.111	0.4875
48.772	0.4827	67.064	0.5182
61.050	0.5081	72.799	0.5302
73.167	0.5461	86.194	0.5711
85.368	0.5703	98.107	0.5960
97.184	0.6048	109.721	0.6539
111.589	0.6510	121.616	0.6679
124.840	0.7202	133.376	0.7163
135.259	0.8091	143.692	0.8754
121.215	0.6712	160.557	1.6718
140.156	0.8614	166.060	2.2016
148.901	1.0211	171.220	1.1629
155.406	1.1697	176.782	0.6356
159.459	1.3972	184.678	0.6568
163.034	1.8125	195.433	0.6565
166.268	1.9370	206.198	0.6533
169.361	1.7069		
171.645	1.3128		
173.772	0.8472		
176.368	0.6655		
180.439	0.6553		
189.139	0.6516		
199.950	0.6612		
211.049	0.6743		

C. Molecular Hydrogen Back Reaction

Through many years of research on the radiation chemistry of polyethylene we have observed indications of a reaction between molecular hydrogen and irradiated polyethylene. At this time we wished specifically to study this reaction, if indeed it exists, and the problem was turned over to Albert G. Mueller, Jr., graduate student and part time research assistant, who has just started to work on the problem.

FUTURE PLANS

A. Specific Heat of High Polymers

We hope to finish the study of polypropylene and then turn either to single crystals of polyethylene, if we can obtain a sufficient quantity of these, or to 10-10 polyamide. We wish to study the polyamide because there is at present in the literature a considerable discrepancy concerning the heats of fusion of polyamides. The estimates vary all the way from 25 to 45 cal. $g.^{-1}$.

B. Radiation Chemistry of Polymers

Many possible amplifications of research in this field could be suggested. Some are as follows:

1. Comparative study of the effect of irradiation in producing degradation and racemization in polypropylene oxide.

2. The molecular hydrogen-irradiated polyethylene back reaction mentioned above. A study of this reaction subsequent to the irradiation might reveal new information concerning the kinetics of chemical effects during irradiation.

3. Electron spin resonance studies of free radicals produced in high polymers, especially polypropylene, by high energy radiations. The investigation of polypropylene was begun a year ago in the summer with the ESR equipment at the Argonne National Laboratory. Thanks to the ARPA grant, we now have our own ESR spectrometer and we intend to start using it shortly. The first use of this equipment will be to test our belief that free radicals decay faster in the presence of molecular hydrogen.

4. Intrinsic viscosity studies of polymers undergoing simultaneous degradation and crosslinking. Here we wish to determine whether or not some mathematical considerations concerning the intrinsic viscosity as a function of radiation dose which we have recently published [J. Phys. Chem., 65, 700 (1961)] are generally valid.

PUBLICATIONS

As yet no papers concerning the research projects supported by MRP-14 have been published. One paper, by Dr. Cracco and the project director, has been written and submitted for publication in the Jour. Amer. Chem. Soc. Its title is, "Radiation Chemistry of Polyethylene. V. Hydrogen Isotope Exchange Studies."

Materials Research Project #15

Effect of Interaction of Imperfections on the Deformation Mechanism

Project Director: J. O. Brittain
Associate Professor, Department of Materials Science

The primary object of this research is to determine the roles played by various point defects on the deformation mechanisms observed in crystalline materials.

In the defect structured intermediate phases NiAl and CoAl a study of the effect of concentration of vacant lattice sites and excess Ni or Co upon creep which was initiated under an NSF grant is being continued (after June 15, 1961) with assistance from ARPA funds. It has already been shown in the NSF sponsored research that the activation energy for creep in NiAl decreases as the composition deviates from the stoichiometric one in either direction. In NiAl the effect is being studied more thoroughly and the range of composition is being extended. A similar study of CoAl is also underway. The creep experiments are of the simple shear type and are being conducted in a vacuum of about 10^{-4} mm of Hg. The technique in the study employs decrements and increments in temperature and stress.

A study of the changes in the active slip systems and deformation mechanism with composition and temperature in iron base alloys was initiated. In Fe-Si alloys, for example, addition of Si reduces the active slip planes from three {110}, {112}, and {123} to one {110}. The object is to study the effect of composition and temperature on the deformation mechanism in other binary and in ternary alloys.

Direct Observation of Lattice Imperfections and their Relation to Mechanical and Physical Properties

Project Director: M. Meshii
Assistant Professor, Department of Materials Science

A. Effect of Electron Irradiation on Mechanical Properties of Metals and Alloys.

K. Cno
M. S. Thesis Research

While the electrical resistivity of electron irradiated metals has been investigated extensively, little attention has been given to changes of mechanical properties. Dixon and Meechan (1953) irradiated copper at 85°K with 5×10^{18} (1.25 Mev) electrons /cm^2 and observed an increase of 25% in hardness. Half of the total change annealed out at 100°C, and the residue at 300°C. They concluded that either interstitials or vacancies can contribute to the hardness. Dieckamp (1955) irradiated large grained 10 mil copper wires at 77°K. No increase in critical shear stress was observed, but there was considerable scatter in the data. More recently, Blewitt and Makin irradiated copper single crystals of 1.5 mm diameter with 4 Mev electrons at room temperature and at liquid nitrogen temperature. The crital resolved shear stress increased from irradiation at both temperatures. No systematic study of the effect of electron irradiation on mechanical properties of metals has been published.

By controlling the beam energy and by studying the recovery of the hardening, it may be possible to separate out the various effects and thus determine the nature of processes causing hardening during and after irradiation.

An apparatus designed for tensile testing and for irradiation at various temperatures between 80° and 300°K has been constructed and its performance is presently being tested. Tensile tests and irradiation can be carried out in the apparatus without transferring the specimen.

Fig. 1 shows the specimen chamber, the stress-strain measuring system, and the cryostat assembled for attaching to the Van de Graaff accelerator.

The cryostat requires about 30 minutes to cool to 80°K. The rate of temperature increase in the specimen chamber has been found to be approximately 10°C per watt. The temperature of the specimen will be below 90°K with 10^{13} 1 to 3 Mev electrons per sec per cm^2.

The stress-strain curve is recorded automatically with a sensitivity of 2 gm/mm^2 and 5 x 10^{-4} for stress and strain, respectively.

Initially the quantitative effects of the electron energy and dose on the magnitude of irradiation hardening will be studied in Al and Cu. Thermal annealing, the influence of the temperature of irradiation and the effect of plastic deformation prior to irradiation will also be investigated. Since the apparatus is designed for both irradiation and tensile testing, the doping effect of preexisting imperfections produced by plastic deformation at various temperatures can be investigated by repeated cycles of extension and irradiation. Quenching studies prior to irradiation may also be included.

Similar apparatus for use to 20°K has been designed and later it is planned to extend the investigation to 20°K where the effect of interstitials on hardening may be particularly interesting.

Along with the mechanical property studies, an electron micrographic study of the defects caused by irradiation is planned. Detection of defects and determination of their behavior at different temperatures and under applied stress will be included here.

B. Electron Micrographic and Mechanical Study of Lattice Imperfections Resulting from Quenching

T. Mori
M.S. Thesis Research

Studies of lattice imperfections by means of electron microscopy and mechanical properties of materials have usually been carried out independently by different groups. It is advantageous to study mechanical properties along with the direct observation of lattice imperfections by an electron microscope. We presently plan to do this combined work on quenched Ag.

The effect of quenching and subsequent aging on the mechanical properties of silver will be determined. Along with this study the structures of the imperfections and their thermal stability will be determined by transmission electron microscopy. The behavior of these defects under an applied stress will also be studied.

According to our previous calculations, the structure and thermal stability of the imperfections resulting from quenched-in vacancies are extremely sensitive to the dislocation and stacking fault energies. The calculation has compared well with the experimental observations in gold. A similar and more thorough check of the theory will be attempted in the present work.

C. Quenching and Aging in Gold-Nickel Alloys

S. S. Chun
M.S. Thesis Research

M. E. Collignon
Undergraduate Research Assistant

It is proposed to study the relation between clustering of quenched-in vacancies and clustering of solute atoms in Au-Ni alloys with the electron microscope.

The process of vacancy clustering and the structure of secondary defects are well understood in pure gold. The present study is an extension of the above work to a gold alloy. Addition of Ni to Au may have a significant effect on vacancy precipitation.

Precipitation of a Ni-rich phase in Au-Ni has been observed by a resistivity change; however, there is no clear understanding of the process.

Mechanisms of hardening from aging after the quench have been proposed in terms of solute atom clustering (or precipitation) in the case of alloys, and vacancy clustering in the case of pure metals. The former mechanism may not be ignored in "pure" metals nor the latter in alloys. The two processes may be interrelated.

D. Quench Hardening in Aluminum

P. W. Shin
Research Assistant

Electron microscope and tensile studies of quench hardening in Al are presently under way. A method has been developed for producing specimens of desired thermal history for direct observation under the electron microscope.

The mechanical testing revealed that the hardening effect due to quenching disappeared partly in the temperature range (160 to 200°C) where prismatic dislocation loops anneal out; however, complete recovery requires a considerably higher temperature. No prismatic dislocation loops exist here. One of the present objects is to determine the cause of hardening which anneals out in the higher temperature region and to clarify the interaction between point imperfections and dislocation lines. It is also hoped to observe the dynamic behavior of prismatic loops under an applied stress and their interaction with gliding dislocations.

Fig. 1 Apparatus for tensile testing in conjunction with irradiation

A. Flange for connecting to Van de Graaff.

B. Transducer for strain measurement.

C. Top of specimen chamber.

D. Liquid nitrogen cryostat.

F. Stress-strain recorder.

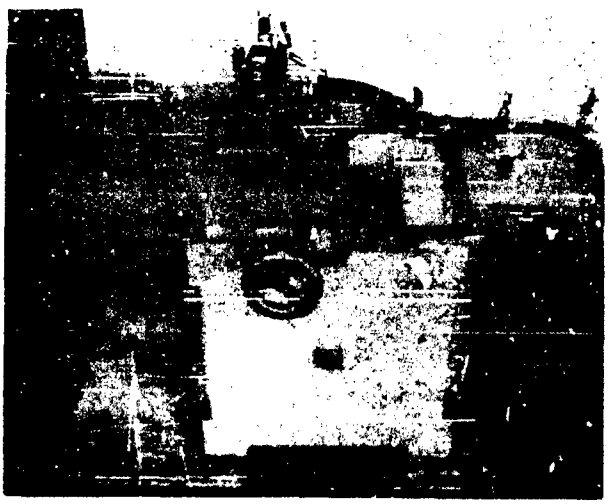

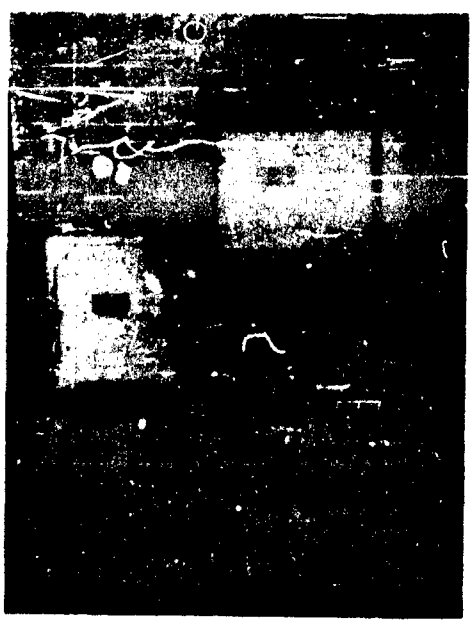

Materials Research Project #17

Nature and Properties of Lattice Imperfections Produced by Electron Irradiation, Quenching, and Low Temperature Deformation.

Project Director: J. W. Kauffman
Associate Professor, Department of Materials Science

INTRODUCTION

The general purpose of this research is to investigate the fundamental nature of structure sensitive properties of materials. An important aspect of this study is the introduction into materials in a controlled fashion of various lattice imperfections, such as lattice vacancies and interstitial atoms. Quenching from high temperatures to low temperatures at controlled rates of cooling is used to introduce lattice vacancies and lattice vacancy complexes into the lattice. Electron irradiation, using the Van de Graaff accelerator, is used to produce simple vacancy interstitial pairs or at higher beam energies multiple vacancy interstitial configurations in materials at low temperature. This facility is a result of a modification of the Van de Graaff accelerator such that it can now produce electrons, as well as positive particles for which the machine was originally designed. This rebuilding of the Van de Graaff has been carried out under AEC support. This research will utilize certain cryostats and other equipment which was built with AEC support.

The research carried out with ARPA support up until about April 1961 was carried out jointly with ONR and AEC. The work was then reorganized so that all subsequent research support with ARPA funds would be carried out with ARPA support alone except for the use of equipment as mentioned above.

A. Recovery of Electrical Resistivity in Gold Quenched from Below 700°C

M. Meshii
Assistant Professor, Department of Materials Science

T. Mori
Research Assistant

Supported in Part by ONR

The residual electrical resistivity at liquid helium temperature of pure gold quenched from temperatures between 700°C and 400°C was determined as a function of annealing time at 62.4°C. On quenching from below 500°C an initial increase in resistivity occurred, followed by the usual decrease with aging time. The time to reach maximum resistivity was found to be a function of the quenched-in resistivity. The increase in resistivity is interpreted as due to vacancy clustering

during the aging process. For quenches above 500°C, clusters form during the quenching process and act as vacancy sinks during subsequent aging. A calculation of the formation of di- and tri-vacancies during the annealing process shows that for a binding energy of 0.3 ev appreciable clustering occurs during annealing after a low temperature quench. A maximum in the calculated concentration of di- and tri-vacancies occurs in the same order of magnitude of time as the observed maximum in resistivity, and is followed by an approximately exponential decay.

B. Resoftening of Quench-Hardened Aluminum

M. Meshii
Assistant Professor, Department of Materials Science

T. Mori
Research Assistant

Supported in Part by ONR

Resoftening of quench-hardened aluminum wire with purity of 99.999 pct was studied. Specimens which had a diameter of 0.016 in. were quenched from 600°C into iced brine and annealed at temperatures between 100°C and 260°C after aging at room temperature for several hours. After this annealing treatment, the yield stress was measured at room temperature. The results are as follows: When the annealing time was 30 min. the annealing temperature at which half of the increase of hardening by quenching and aging was eliminated was 200°C, and more than 260°C was necessary to anneal the specimen into fully softened condition. Isothermal annealings which were performed at 170°C to 230°C showed that the activation energy for resoftening was about 1.2 ev. The temperature dependence of the yield stress was higher for the quenched specimens than for the annealed ones.

Neither the rate nor the temperature of resoftening corresponds to the rate or temperature of disappearance of prismatic dislocation rings as observed by electron microscopy. Therefore, prismatic dislocation loops may not be a major source of quench-hardening in aluminum.

C. Effect of Quenching Rate on the Quenched-in Resistivity in Gold

M. Meshii
Assistant Professor, Department of Materials Science

T. Mori
Research Assistant

Supported in Part by ONR

The effect of quenching rate on the quenched-in resistivity in gold

was experimentally studied. For quenching temperatures of 1030°, 900°, 800°, and 700°C a linear relation between the logarithm of the quenched-in resistivity and the reciprocal of the quenching rate was found. (The investigated range was 10^4 to 8×10^4°C/sec.) The quenched-in resistivity, $\rho_\infty = A \exp(-E_F/kT)$, where $A = 5.0 \times 10^{-4}$ ohm-cm and the formation energy, $E_F = 0.97$ ev. Using measurement of the volume change of quenched specimens and assuming that a vacancy has 0.4 atomic volume, the following constants were obtained: The resistivity of one atomic percent of vacancies is 1.4×10^{-6} ohm-cm; the entropy of formation of a vacancy is 1.1×10^{-4} ev/°K; and the fractional concentration at the melting point is 7.5×10^{-4}.

D. Electrical Resistivity Recovery Above -80°C in Electron-Irradiated Gold

R. A. Vullaert
M.S. Thesis Research

Supported in Part by AEC

Gold wire of 99.999% purity was irradiated with 2.4-Mev electrons at about 110°K; the electrical resistivity was measured at 4.2°K following various isochronal and isothermal anneals at temperatures above -80°C. In the isochronal recovery, two major processes were evident between -80°C and the temperature at which complete recovery occurred (+160°C). Stage II recovery was observed up to about -25°C and the fractional recovery corresponds closely to that for irradiations carried out with the specimen temperature near 10°K.[1] Appreciable stage III recovery extended from about -10° to +100°C. Activation energies were determined by the slope intersection method for stage III recovery. The average of eight determinations at temperatures between -50 and +75°C was 0.66 ± 0.05 ev.

E. Theoretical Calculations of Vacancy Migration and Coagulation

One of the most widely used methods for the study of the properties of lattice imperfections is the study of the rate of resistivity change due to isothermal reduction in the supersaturated concentration of defects. Attempts at the analysis of this type of data are usually made first in terms of a simple activation energy even though the activation energy may be variable and secondly in terms of the order of the reaction. It has been found that often such a simple approach to the analysis of the data is not adequate, and one must assume that more complicated processes occur involving various activation energies.

[1] J. B. Ward, Ph.D. thesis, Northwestern University, 1960.

Besides the simple process of individual lattice vacancies migrating to fixed sinks, other processes appear to be important: these are the coagulation of vacancies to form di-vacancies, tri-vacancies and under certain conditions large complex configurations, such as tetrahedral stacking faults. It has been shown [Meri, Meshii and Kauffman, Philosophical Magazine 5, 687 and 939 (1960)] that these complexes are important and that they produce a large effect on the mechanical properties of quenched gold. The present calculations involve the following processes: 1) The migration of single vacancies and di-vacancies to fixed random sinks, 2) the formation and destruction of di-vacancies as a result of vacancy-vacancy collisions, and 3) the formation and breakup of tri-vacancies as the result of di-vacancy single vacancy collisions. These processes may be represented by the following chemical equations:

$$V_2 \rightarrow N \quad \text{sinks}$$

$$V_3 \rightarrow N \quad \text{sinks}$$

$$V_1 + V_1 \rightleftharpoons V_2$$

$$V_1 + V_2 \rightleftharpoons V_3$$

These chemical equations, under the assumption that the various components remain random throughout the process, result in the following three simultaneous differential equations:

$$\frac{dC}{dt} = -NC\nu e^{-\varepsilon_1/kT} - 2\gamma_{11}C^2\nu e^{-\varepsilon_1/kT} + 2\gamma'_{21}C_2\nu e^{-(\varepsilon_1+B)/kt} - \gamma_{13}CC_2\nu e^{-\varepsilon_2/kT} + \gamma'_{31}C_3\nu e^{-(\varepsilon_2+B')/kT}$$

$$\frac{dC_2}{dt} = -NC_2\nu e^{-\varepsilon_2/kT} - \gamma_{11}C^2\nu e^{-\varepsilon_1/kT} - \gamma'_{21}C_2\nu_3 e^{-(\varepsilon_1+B)/kT} - \gamma_{13}CC_2\nu e^{-\varepsilon_2/kT} + \gamma'_{31}C_2\, e^{-(\varepsilon_2+B')kT}$$

$$\frac{dC_3}{dt} = +\gamma_{13}CC_2\nu e^{-\varepsilon_2/kT} - \gamma'_{31}C_3\nu e^{-(\varepsilon_2+B')/kT}$$

C_1, C_2, C_3 are the concentration of single, di and tri-vacancies, the γs and γ's are the combinatory numbers for association and disassociation of vacancies, and B_1 and B' are the binding energies.

These equations have been solved numerically, using a 650 IBM Digital Computer. Various sink densities, (N), various concentrations (C_1,C_2,C_3), and various binding energies (B_1 B') were used in the calculations. The main results of these calculations to date indicate that upon annealing there is a very rapid transient condition under which many di-vacancies and tri-vacancies are formed. The maximum value of the concentrations of these complexes as well as the time to reach the maximum concentrations are influenced by the sink density. After the rapid transient a long steady-state decay occurs, which apparently continues until the process reaches equilibrium. Some of these results are included in the paper: "Recovery of Electrical Resistivity in Gold Quenched from Below 700°C," which has been accepted for publication in the Physical Review. Recent experimental results of vacancy migration in quenched gold and recovery of electrical resistivity in irradiated gold are being studied in terms of the calculations. It is hoped that this study will aid in the understanding of the processes which occur upon room temperature annealing. These processes are at present not understood and there is considerable disagreement among the various groups studying radiation damage.

Recent experimental results (R. Kloske, M.S. Thesis, Northwestern University: now in preparation) indicate that impurities play an important role in determining the nature of the annealing kinetics and it is hoped that these calculations may be extended to include impurity-vacancy interactions.

F. Electron Irradiation of Quenched Gold

J. A. Tesk
Ph.D. Thesis Research

The essential idea of this experiment is that by introducing an excess of vacancies by quenching additional sinks for interstitial atoms result. Since no previous study of this type has been carried out the precise objectives and methods of analysis can not be definitely stated at this time, but it is expected that interesting and valuable information regarding the nature of the migration of interstitial atoms will result. It should also be possible to control to some extent the formation of interstitial clusters by controlling the concentration of quenched-in lattice vacancies. It is hoped to be able to make quantitative estimates of the distance of migration of interstitial atoms and learn something of the nature of the various processes.

PUBLICATIONS

Recovery of Electrical Resistivity in Gold Quenched from Below 700°C. Now being revised before final publication in The Physical Review. T. Mori, M. Meshii and J. W. Kauffman.

Resoftening of Quench-Hardened Aluminum, J. of Metals, Vol. 13, 82 (1961) T. Mori, M. Meshii and J. W. Kauffman. (Abstract)

The Effect of Quenching Rate on the Quenched-in Resistivity in Gold, Bull. Am. Phys. Soc. II, 6, 157 (1961) T. Mori, M. Meshii and J. W. Kauffman. (Abstract)

Electrical Resistivity Recovery Above -80°C in Electron Irradiated Gold, Bull. Am. Phys. Soc. II, 6, 157 (1961) R. Wullert and J. W. Kauffman. (Abstract)

Surface Chemistry of Metals and Oxides

Project Director: P. W. Selwood
Professor, Department of Chemistry

A. The Effect of Hydrogen on the Magnetization of Nickel

The sorption of hydrogen on small particles of nickel takes place in two stages: first, a virtually instantaneous, non-activated chemisorption, and second, a slow process, the precise nature of which has remained obscure. The several suggestions which have been made to explain this phenomenon include:

1) The slow process represents an activated adsorption. This is to say that an activation energy is required to bring about the sequence of steps leading from molecular hydrogen to formation of the nickel-hydrogen bond[1].

2) The slow process is nothing more than a slow chemical reduction of superficially oxidized nickel[2].

3) The action of the hydrogen on the nickel surface is to create adsorption sites, the formation and decay of which determine the adsorption rate[3].

4) The rate-determining process is diffusion of hydrogen into less accessible particles of metal[4].

5) The slow process represents "dissolving" of hydrogen in the metal[5].

Measurements of magnetization as a function of hydrogen uptake have shown that the slope of the isotherm relating magnetization to volume of gas adsorbed may be different for the fast and slow processes. The theory of this difference has been worked out on the assumption that the slow process rate is diffusion-controlled and that there is otherwise no intrinsic difference between fast and slow sorption. This makes it possible to calculate the total volume of nickel which is active in each of the two steps, and also to calculate the average volumes of the particles involved.

For ferromagnetic particles in the superparamagnetic diameter range[6], the magnetization M at low field, H, and moderate temperature, T, is given by the low-field approximation to the Langevin function:

$$M = N \frac{(I_{sp}v)^2 H}{3kT}$$

where N is the total number of particles of volume v, and I_{sp} is the spontaneous magnetization.

After adsorption of vapor molecules on a particle surface, the magnetic moment ($I_{sp}v$) of the particle becomes ($I_{sp}v - n_H\varepsilon\beta$), where n_H is the number of hydrogen atoms adsorbed per particle; ε is the change of moment produced by one hydrogen atom, expressed in Bohr magnetons; and β is the Bohr magneton.

Then, after adsorption, we have:

$$M' = N \frac{(I_{sp} - n_H \varepsilon\beta)^2 H}{3kT}$$

and

$$\frac{\Delta M}{M} = \frac{-2n_H \varepsilon\beta}{I_{sp}v} + \left(\frac{n_H\varepsilon\beta}{I_{sp}v}\right)^2$$

As $\Delta M/M$ rarely exceeds 0.15 we may ignore the squared term.

If now we have a system containing two sizes of particles of volume v_1, and v_2, then:

$$\frac{\Delta M_1/M_1}{\Delta M_2/M_2} = \frac{n_{H(1)}\ v_2}{n_{H(2)}\ v_1}$$

and, inasmuch as M_1 and M_2 may be expressed as functions of N_1 and N_2, we may write

$$\frac{\Delta M_1}{\Delta M_2} = \frac{n_{H(1)}\ V_1}{n_{H(2)}\ V_2}$$

where V = Nv, that is to say, the total volume of ferromagnetic matter in the sample.

If we assume that the individual particles are spheres (an assumption for which there is some evidence), then the relative volumes of these particles may be related to the hydrogen adsorbed by each process:

$$\frac{N_{H(1)}}{N_{H(2)}} = \frac{N_1 v_1^{2/3}}{N_2 v_2^{2/3}}$$

where N_H is the total number of hydrogen atoms taken up by all particles of a given size.

Finally we may substitute in our expression for $\Delta M_1/\Delta M_2$ and obtain:

$$\frac{\Delta M_1}{\Delta M_2} = \left(\frac{N_{H(1)}}{N_{H(2)}} \right)^{5/2} \left(\frac{N_2}{N_1} \right)^{3/2}$$

From the above expressions one may calculate N_1/N_2, v_1/v_2, and M_1/M_2 by substitution of the experimental data. The results for a typical nickel preparation are as follows:

$\Delta M_1/\Delta M_2$ (obs.)	30
$N_{H(1)}/N_{H(2)}$ (obs.)	12.4
N_1/N_2	7.05
v_1/v_2	2.34
V_1/V_2	16.5
M_1/M_2	38.6

The average diameter of the larger particles is 60Å.

This method has been applied to several different preparations. All show the internal consistency of the calculations given above. The conclusion is, therefore, that there is no intrinsic difference between "fast" and "slow" sorption of hydrogen on nickel, and that the rate determining process is probably diffusion.

It is believed that this work clears up an old controversy concerning the nature of the slow process. It also suggests a correlation between the "solubility" of hydrogen in pure polycrystalline nickel and the well-known anomalous approach to magnetic saturation at room temperature.

The work is expected to be completed by August or September 1961.

REFERENCES

1. H. S. Taylor, J. Am. Chem. Soc. 53, 578 (1931)

2. G. C. A. Schuit and N. H. De Boer, Rec. Trav. Chim. Pays-Bas 72, 909 (1953).

3. L. Liebowitz, H. J. D. Low, and H. A. Taylor, J. Phys. Chem. 62, 471 (1958).

4. W. A. Doerner, Dissertation, University of Michigan (1952).

5. D. P. Smith, Hydrogen in Metals, University of Chicago Press, Chicago (1948). Professor Smith describes the several earlier points of view and presents the evidence pro and con.

6. C. P. Bean and J. D. Livingston, J. Applied Phys. 30S, 120S (1959).

Stress Distribution in Visco-Elastic Media - Thermal Stress Problems

Project Director: O. C. Zienkiewicz
Professor, Department of Civil Engineering

The initial objectives of the proposed research are: (a) general formulation of visco-elastic stress analysis problems in terms suitable for numerical or analogue solutions; (b) development of slab analogy methods.

A procedure for formulating visco-elastic thermal stress problems in terms of equivalent temperatures applied to an elastic problem has been developed for materials which exhibit a constant Poisson's ratio but in which the properties are functions of time. A paper entitled, "The Analysis of the Visco-Elastic Behavior of Concrete Structures - with Particular Reference to Thermal Stresses", which has been accepted for publication by the American Concrete Institute, describes some of the concepts introduced.

The experimental analogue method of slab analogy to which the Moire Technique was applied has proved successful in dealing with thermo-elastic plane problems. A description of the preliminary experiments, and verification of the method against known results, is described in a paper entitled, "The Use of Slab Analogy in the Determination of Thermal Stresses" which was submitted for publication in May 1961. This paper describes also the extension of the analogy to some visco-elastic problems. Intensive work on the improvement of apparatus and technique is in progress and will be continued through the summer of 1961.

This research project will terminate in September 1961 since the principal investigator is taking up the Chair of Civil Engineering at the University of Wales, Great Britain.

PUBLICATION

1. "The Analysis of the Visco-Elastic Behavior of Concrete Structures with Particular Reference to Thermal Stresses". (Accepted for publication, April 1961 by American Concrete Institute).
2. "The Use of Slab Analogy in the Determination of Thermal Stresses". (Submitted for publication in Journal of Mechanical Engineering Science, May 1961).

Materials Research Project #20

Low Temperature Specific Heats of Alloy Phases

Project Director: D. H. Whitmore
Associate Professor, Department of Materials Science

D. Rajdev
Research Assistant

Earlier work in this laboratory by R. F. Janninck (M.S. Thesis) has indicated the possibility of a strong contribution to the specific heat from an additional linear term, $\gamma'T$, in Ag-rich, Ag-Cd solid solutions near an electron-atom ratio of 1.2. The occurrence of this term is in agreement with a theoretical prediction by H. Jones [Proc. Roy. Soc. (London) A240, 321 (1957)] that such a linear additional contribution would arise whenever the Fermi surface of the alloy is in close proximity to the Brillouin zone boundary.

In order to verify and study the effect further the low-temperature calorimeter has been modified and Ag-rich, Ag-Cd solid solutions in the range where the strongest electron-phonon interactions are expected (about 20 atomic % Cd) have been prepared. The equipment modifications include a redesign of the calorimeter can to facilitate introduction of the sample and some changes in the vacuum system for evacuating the calorimeter can. Four additional alloy compositions near 20 atomic % Cd have been prepared. They were melted in an inert atmosphere and then annealed for about two weeks at temperatures immediately below the alloys' solidus temperatures. The calorimeter has been checked out and the measurements are in progress.

Materials Research Project #21

The Study of Rates of Very Rapid Chemical and Physical Processes by Means of NMR and EPR

Project Director: R. G. Pearson
Professor, Department of Chemistry

A fairly detailed study has been made of the interaction of different paramagnetic ions in aqueous solution by means of the EPR line broadening. For cations interacting with anions, a theory has been developed which postulates that the chief interaction comes during the life-time of an ion-pair or outer sphere complex. The line broadening then gives a lower limit to the rates of formation and dissociation of such ion-pairs. In a number of cases the rates have clearly been measured.

The results agree with the theory for diffusion-controlled reactions between ions in solution. Life-times of 10^{-7} - 10^{-8} seconds are easily measured by the EPR method.

It is hoped to continue work on this project next year.

To date this research has been supported by ARPA only to the extent of furnishing the electron paramagnetic resonance unit.

A paper, "Paramagnetic Relaxation in Solutions," coauthored with Dr. T. Buch, Instructor in Chemistry, on the theory and experiment is being given at the June, 1961 meeting of the American Physical Society in Mexico City.

Materials Research Project #22

The Effect of Phonon Bombardment on the Conductivity and Photoconductivity of Crystal Phosphors

Project Director: J. E. Jacobs
Professor, Department of Electrical Engineering

T. A. Kriofsky
Graduate Research Assistant
M.S. Thesis Research

INTRODUCTION

The purpose of this study is: 1) to investigate the effects of phonon bombardment in the form of ultrasonic waves on the conductivity of pure and photosensitive crystals of sulfides, selenides and tellurides of cadmium and zinc, under varying light conditions, and 2) to present a model for the conduction mechanism.

Large increases in conductivity have been observed during phonon bombardment. A major portion of these changes may be accounted for thermally; however, there does not appear to be a one-to-one correspondence between the purely thermal effect and the effect due to the ultrasonic field.

In the process of absorption of an ultrasonic wave, heat is released, both in the medium of transmission and in the medium in which the wave is terminated. Thus, it is expected that some thermal effect on conductivity should be apparent (for example, thermally induced lattice vibrations, or absorption of thermal energy by electrons). This effect has been reported by Zhuravlev and Kozak[1] as an increase in conductivity and has been verified by experiments completed thus far.

Electrons moving through a crystal lattice interact with the atoms of the lattice. In the process of collision they lose some of their energy and experience a change in direction of motion. The energy lost causes a periodic expansion and contraction of the lattice which travels through the lattice structure at the speed of sound (that is, a phonon is created). Similarly, an electron may absorb energy from a phonon. Normally this effect is small, and it is usually neglected in calculations. However, by bombarding the crystal with phonons in the form of ultrasonic waves, the absorption of phonon energy by electrons may be increased, an occurrence which may account for an increase in conductivity.

In photosensitive materials, trapping of carriers by impurity centers is a major factor in limiting the conductivity, as trapping decreases the lifetime of the carriers and thereby decreases the conductivity. It is feasible that phonon bombardment may keep these trapping centers vacant and thus increase the carrier lifetime and the conductivity.

The effect of ultrasound on the conductivity and photoconductivity of phosphors has not been studied extensively; however, some theories have been advanced in an attempt to explain experimental results[1,2,3]. It was intended in this investigation to attempt to verify these reports in regard to pure crystals, and to further investigate the properties of crystals containing impurities and activators under phonon bombardment. Photoconductive crystals of CdS (with known concentrations of Ag, Cu, Al, Mn, or Hg impurities), CdTe, CdSe, and ZnS are available for study.

EXPERIMENTAL

The studies are being conducted both 1) on crystals which have had no special surface preparation and 2) on crystals which have been cleaned and prepared by a method described by Greiner[4] which consists of subsequent washings of the samples in HCl, distilled water, and alcohol, and then drying them in air. This latter method has not proven successful in all cases, since the air drying causes a decrease in photosensitivity. At present no facilities are available for vacuum drying.

Two types of electrodes are employed. Initial experiments were conducted with a colloidal carbon as the contact material. These contacts were noisy and non-ohmic at low voltages but became ohmic above 20 to 25 volts. A second method of attaching electrodes involves the use of indium to make contact to the crystal and then conductive silver paint or colloidal carbon to attach the electrodes to the indium. The indium contacts are preferred, since ohmic behavior is obtained even at very low voltages and contact noise is greatly reduced. Evaporation techniques were found to be the most satisfactory for depositing the indium on the crystals.

The crystals are fixed to a thin glass disk with a non-conducting epoxy cement. A copper-constantan thermocouple is also imbedded in the epoxy and is in contact with the crystal. Thus an indication of the temperature of the crystal is obtained. The disk is sealed watertight to the end of a pyrex tube and is immersed in the liquid which is used to transmit the ultrasound.

The crystals are exposed to 1 Mc/sec ultrasound intensities up to approximately 5 watts/cm^2 transmitted through water.

The crystals are excited with white, red, green and blue light, and the photoconductivity is observed before and after exposure to the ultrasonic field. In order to minimize noise, the light source is operated with direct current.

Conductivity-temperature response curves are taken by heating the crystals slowly and simultaneously recording temperature and current. Then the crystals are irradiated with an ultrasonic field (under various light conditions), and again temperature and current are recorded simultaneously. This result is compared to the temperature response

curve obtained purely from heating. Also, the increasing conductivity as a function of temperature obtained during phonon bombardment is compared to the decaying conductivity as a function of temperature after removing the ultrasonic field.

RESULTS AND CONCLUSIONS

Although the experiments have not yet been completed, in general the following trends have been observed.

In pure crystals of CdS, CdSe, and CdTe, the increase in dark conductivity during phonon bombardment has been small and appears to be entirely thermal. Changes in photoconductivity have been observed, although they have not been reproducible to the extent desired.

In CdS crystals containing impurities larger increases in conductivity have been observed (20x to 100x) during phonon bombardment. The effect does not appear to be entirely thermal. The energy band gap of a typical crystal (aluminum activated) has been calculated from a plot of conductivity vs. temperature. In the absence of phonon bombardment a value of 0.3 electron volts was found. The low gap voltage indicates that the conductivity is impurity dominated. However, if a plot is made of conductivity during phonon bombardment vs. temperature a higher gap voltage is obtained. This behavior indicates the presence of some effect other than thermal.

Photoconductivity in the activated CdS has in some cases increased and in other cases decreased during phonon bombardment. Therefore, the presence of a non-thermal process is suspected.

The following conclusions and speculations may be offered:

In pure crystal phosphors the effect of phonon bombardment on the conductivity is due almost exclusively to the heat produced by absorption of the ultrasonic wave.

In crystals containing impurities and activators, there appears to be an effect causing an increase in conductivity in addition to that due to heat. The mechanism of this effect remains to be determined and is the object of further study.

REFERENCES

1. Zhuravlev, V.A., and Kozak, M.L., "The Conductivity of Semiconductors in an Ultrasonic Field"; Zh. Eksper. Teor. Fiz., 36, 343-4, (1959).

2. Herforth, L., and Krumbiegel, J., "The Effect of Ultrasound on the Conductivity and Fluorescence of Zinc and Cadmium Sulphide Crystals"; Naturwissenschaften, 42, 39, (1955).

3. Nine, Harmon D., "Photosensitive Ultrasonic Attenuation in CdS"; Physical Review Letters, 4, 359-61, (1960).

4. Greiner, R. A., Miller, R. F., and Rutherford, R.C., "Effects of Electrode Materials and Surface Preparation on CdS-Metal Contacts"; Journal of Applied Physics, 28, 1358-9, (1957).

Heterogeneous Nucleation From Surface Cavities

Project Director: S. G. Bankoff
Professor, Department of Chemical Engineering

Heterogeneous nucleation, in which the phase transition is catalyzed by the presence of external surfaces, is a general mechanism for many phase transitions. Because of the presence of the small imperfections in the external surface, embryos of the new phase can exist metastably under free energy conditions which would lead to their rapid disappearance in the homogeneous system. The process is of extreme importance in solid-solid and solid-liquid phase transformations, but unfortunately experimental conditions in these systems do not allow easy study of the nucleation surfaces.

A system which may be readily studied under reproducible conditions, however, is the nucleation of vapor from a solid surface. In this case, as well as freezing and melting of liquids, small crevices in the surface represent the nucleation sites, while the surface temperature required for nucleation specifies the excess free energy characteristic of each site. Hence, it is possible to get a direct confirmation of heterogeneous nucleation theory not possible with other systems by measurement of the diameter of nucleation imperfections and comparison of these geometric quantities with theory. It is proposed to use a cast or highly polished surface, such as glass, which has been gold-plated in order to allow easier identification of nucleation sites. Dimensions of nucleation sites, measured by microphotography, will be used, in conjunction with measurements of surface temperature required just to initiate bubble nucleation from that particular site, to test the theory. In addition, it is proposed to obtain the distribution functions for these imperfections on carefully characterized surfaces. Later the experimental work may be extended to freezing and melting of transparent materials.

Experimental work has not yet been initiated.

Surface Ionization Phenomena

Project Director: A. B. Cambel
Professor, Department of Mechanical Engineering

J. F. Wendt
M. S. Thesis Research

The purpose of this study is to improve the understanding of the phenomenon of surface ionization. The particular project now being developed calls for the ionization of potassium vapor on a thin tungsten filament. The work function will be determined as a function of the vapor pressure of potassium.

For this purpose an almost completely glass system was designed and constructed. The glass experimental tube is fitted with three nickel electrodes drilled with an 0.080 in. hole through which passes a 0.002 in. diameter tungsten filament, spring loaded. The tube also contains a reservoir for the liquid potassium which is necessary to provide a controlled atmosphere of potassium vapor. An ionization gauge vacuum tube also has been mounted in the system for reading pressures in the 10^{-4} to 10^{-7} mm Hg range. This tube will be sealed off prior to an experimental run.

The new system seems to operate properly and leak testing runs are being made at the present time. It is hoped that experimental runs will be started soon.

Contract SD-67 financial support of this research went into effect June 15, 1961.